Control Theory for Gain Scheduling

Overview

A major advantage of gain scheduling control is that it provides *nonlinear* parameter-dependent systems a *nonlinear* time varying controller by using *linear* time invariant ones. It has been remarked that for real world applications the elegant and powerful results of the modern $\mathscr{H}_\infty$ control theory are particularly interesting for the synthesis of LTI controllers in contrast to other methods such as predictive and/or pure nonlinear control strategies that risk being overly complex and/or difficult to implement. In this work two $\mathscr{H}_\infty$ control structures were tested in order to provide the necessary LTI controllers needed for interpolation in the gain scheduling control context. This chapter offers a solid yet not exhaustive review of two of these methods: $\mathscr{H}_\infty$ dynamic output feedback with pole placement constraints and $\mathscr{H}_\infty$ dynamic and static loop shaping. In addition some rather standard results concerning full order state observers and Youla parametrization (in use with the first synthesis method) and an important system analysis tool called the *gap metric* (in use with the second synthesis method) are presented.

Chapter contents

3.1 $\mathscr{H}_\infty$ Control in LMI Regions

In this section some theoretical results concerning $\mathscr{H}_\infty$ control with pole placement constraints in LMI regions will be presented. The section starts with a classical analysis motivating the use of this powerful synthesis method for the computation of LTI controllers at the first benchmark example of Chapter 5. The subsequent sections give all the necessary results for a systematic treatment of this control problem with most of the material drawn from [27].

3.1.1 Motivation

2^{nd} order system analysis

Consider a SISO linear time invariant system $G(s)$ and a controller $K(s)$ in a standard closed loop control configuration (see Fig. 3.1a). The primary goal of classical control systems is to design the controller K so that the time response $y(t)$ to a step reference input $y_\mathrm{r}(t)$ has *good* properties. Many of these properties are dominated mostly by the location of the poles λ of the closed loop system $H(s)$ with:

$$H(s) \triangleq \frac{Y(s)}{Y_\mathrm{r}(s)} = \frac{G(s)K(s)}{1 + G(s)K(s)} \tag{3.1}$$

To quantify the influence of the pole location to the time response of the closed loop system $H(s)$, suppose that H is or may be approximated by a second order system (see Fig 3.1b), as is the case very often in practice, with:

$$H(s) = \frac{\omega_\mathrm{n}^2}{s^2 + 2\xi\omega_\mathrm{n}s + \omega_\mathrm{n}^2} \tag{3.2}$$

The transfer function parameters ω_n and ξ are called *undamped natural frequency* and *damping ratio* of the poles $\lambda_{1,2}$ of H, being the roots of its denominator, with:

$$\lambda_{1,2} = -\xi\omega_\mathrm{n} \pm j\omega_\mathrm{n}\sqrt{1-\xi^2}. \tag{3.3}$$

Poles

The quantitative meaning of the two fundamental variables ω_n and ξ is related to the step response of H. The undamped natural frequency is the system's output oscillation frequency if its damping ratio is reduced to zero whereas the damping ratio is closely related to the overshoot experienced on the system's step response, given that the system is underdamped.

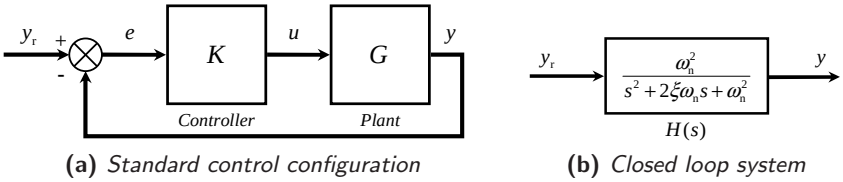

(a) *Standard control configuration* **(b)** *Closed loop system*

Figure 3.1: Basic analysis block diagrams.

Damping scenarios

The poles $\lambda_{1,2}$ depend on both ω_n and ξ (see Eq. 3.3), but it is the latter that characterizes the form of the step response $y(t)$. Four scenarios are considered for the damping ratio: $\xi = 0$ (non-damped), $0 < \xi < 1$ (underdamped), $\xi = 1$ (critically damped) and $\xi > 1$ (overdamped). The first and the third scenarios may be considered as limit cases of the second and the fourth ones.

In the non-damped case ($\xi = 0$) the closed loop poles are purely imaginary with $\lambda_{1,2}^{nd} = \pm j\omega_n$ and the time response is purely oscillatory whereas in the critically damped case ($\xi = 1$) the closed loop poles are purely real and negative with equal values $\lambda_{1,2}^{cd} = -\omega_n$. The system in the first case is said to be *conditionally stable* whereas in the second remains always *stable*. In the overdamped case ($\xi > 1$) the system demonstrates two distinct stable real poles with $\lambda_{1,2}^{od} = (-\xi \pm \sqrt{\xi^2 - 1})\omega_n$. For a constant undamped natural frequency, as the damping ratio increases the first stable pole goes to infinity whereas the second goes to zero. Thus, the time response of such as system becomes sluggish since it gets dominated by a slow stable eigenvalue. All three cases are not interesting for a control system for stability and/or speed reasons, so only the underdamped case is considered in the following analysis.

For an underdamped system $0 < \xi < 1$ its step response $y(t)$ and step tracking error $e(t) = y_r(t) - y(t)$ (see Fig. 3.1b) are computed using basic knowledge of ODE theory as (see [105], pp. 147-148)[1]:

$$y(t) = 1 - \frac{e^{-\xi\omega_n t}}{\sqrt{1-\xi^2}} \sin\left(\omega_d t + \arctan\frac{\sqrt{1-\xi^2}}{\xi}\right) \tag{3.4}$$

$$e(t) = e^{-\xi\omega_n t}\left(\cos\omega_d t + \frac{\xi}{\sqrt{1-\xi^2}}\sin\omega_d t\right). \tag{3.5}$$

The step response $y(t)$ of $H(s)$ for a given ω_n, presents different amounts of overshoot and oscillation around the desired reference trajectory $y_r(t)$ for different values of ξ (see Fig. 3.2a) whereas its settling speed for a given ξ is a function of ω_n (see Fig. 3.2b).

In order to characterize an LTI system in a more uniform way, several properties of its step time response $y(t)$ may be defined, depending only on the damping ratio ξ and undamped natural frequency ω_n. Some of these properties are the *rise time* t_r, *peak time* t_p, *settling time* t_s and *overshoot* M_p (see Fig. 3.2c) and may be easily calculated for a second order system as:

Step response properties

1. *Rise Time* t_r*:* It is usually defined as the time that the step response $y(t)$ takes to reach its 100% value for the first time. It may be computed from Eq. 3.4 by letting $y(t) = 1$:

$$t_r = \frac{\pi - \arctan\dfrac{\sqrt{1-\xi^2}}{\xi}}{\omega_n\sqrt{1-\xi^2}}. \tag{3.6}$$

[1] The quantity $\omega_d = \omega_n\sqrt{1-\xi^2}$ is called the *damped* natural frequency.

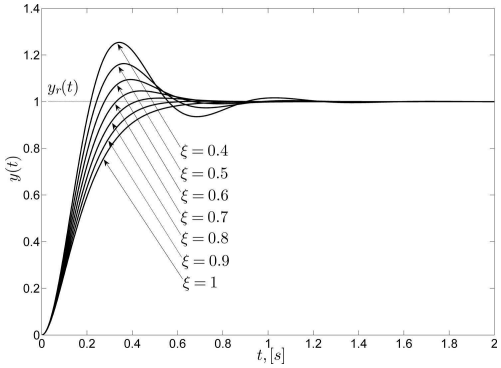

(a) *Step responses (varying ξ)*

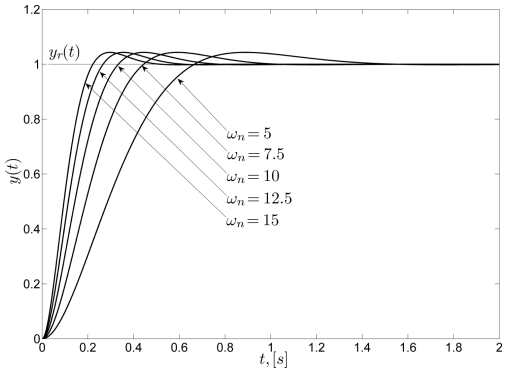

(b) *Step responses (varying ω_n)*

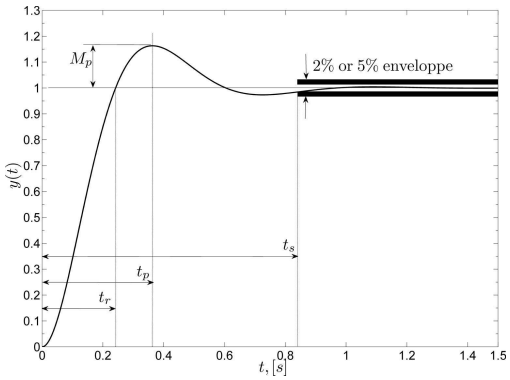

(c) *Step response characteristics*

Figure 3.2: Step response study - *underdamped case*.

2. *Peak Time* t_p*:* It is defined as the time that the step response $y(t)$ takes to reach its maximum value. It is computed by letting the derivative of $y(t)$ go to zero:

$$t_\mathrm{p} = \frac{\pi}{\omega_\mathrm{n}\sqrt{1-\xi^2}} = \frac{\pi}{\omega_\mathrm{d}}. \tag{3.7}$$

3. *Settling Time* t_s*:* It is defined as the time that the step response $y(t)$ takes to reach a 2% or 5% envelope around its steady state value $y(t_\infty)$. It is approximatively computed as:

$$t_\mathrm{s} = \frac{3}{\xi\omega_\mathrm{n}} \quad (5\% \text{ criterion}) \tag{3.8}$$

$$t_\mathrm{s} = \frac{4}{\xi\omega_\mathrm{n}} \quad (2\% \text{ criterion}) \tag{3.9}$$

4. *Maximum Overshoot* M_p*:* It is defined as the maximum positive percentage deviation (occurring at the peak time $t = t_\mathrm{p}$) of the step response $y(t)$. It is computed as:

$$M_\mathrm{p} = \frac{y(t_\mathrm{p}) - y(t_\infty)}{y(t_\infty)} \cdot 100\% = e^{\frac{-\pi\xi}{\sqrt{1-\xi^2}}} \cdot 100\% \tag{3.10}$$

Pole placement discussion

A control system should be able to provide satisfactory *response times* and *damping* for the plant under control. For a second order system with the simple form of Eq. 3.2, this is done by placing its poles $\lambda_{1,2}$ (see Eq. 3.3) to an appropriate location following two rules of thumb, as it has been implied in the preceding analysis: first the desired settling time t_s of the process is set by adjusting the undamped natural frequency ω_n and then an appropriate damping ratio ξ is chosen in order on the one hand avoid excessive overshoot, and on the other hand obtain a time response for the system that is not too sluggish.

The dependence of the rise, peak and settling times over the damping ratio and a given undamped natural frequency is shown in Fig. 3.3a[2]. Even though the rise and peak times augment monotonically with the damping ratio ξ, it does not happen the same with the settling time. It may be remarked that while the settling time is almost constant for medium values of the damping ratio $0.45 \leq \xi \leq 0.65$, it reaches a minimum for $\xi \simeq 0.69$ and then starts to rise almost linearly. The corresponding percentage overshoot M_p for this optimal value of the damping ratio is about 4.7% (see Fig. 3.3b). In practice, a damping ratio between 0.6 and 0.8 for the closed poles of a real-world system is considered satisfactory with the undamped natural frequency being chosen as a function of the specific bandwidth demanded from the control system.

[2]The figure shows the settling time for $\omega_\mathrm{n} = 1 rad/s$ and thus provides scaling for any ω_n.

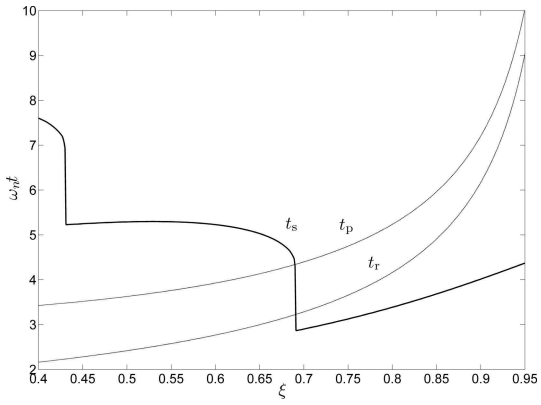

(a) *Step response times*

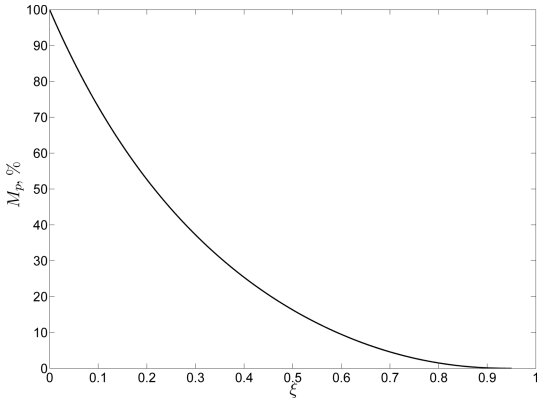

(b) *Step response overshoot*

Figure 3.3: Step response characteristics.

3.1.2 LMI Regions

Motivation for eigenvalue clustering

From the analysis of the previous section it has been made clear that the transient behavior of a control system is dominated by the location of its closed loop poles. For a simple second order system as the one in Eq. 3.2, it is generally easy to obtain the desired closed loop dynamics by setting the damping ratio and undamped natural frequency to some desired values. For a higher order system there exist also solid methods for robust state/output feedback eigenvalue placement to an arbitrary accuracy (see for example [72] for details on the algorithm implemented in MATLAB® for state feedback eigenvalue placement).

Besides focusing on eigenvalue placement only, a control system could provide a control law that takes into account constraints over frequency domain aspects, robustness over external perturbations and parametric uncertainties. A good way to take into account all these requirements is the $\mathscr{H}_\infty$ robust control context with additional eigenvalue placement constraints. There exists an extensive literature over this general problem of *root clustering* (e.g. see [28, 56, 57]); here however the approach found in [27] will be preferred since the author believes that it gives the more general results on the subject. Having given the motivation why eigenvalue placement is so important in Section 3.1.1, this section presents some introductory material over the famous LMI regions.

3.1.2.1 Design Objectives

As pointed out in the previous analysis, an eigenvalue placement procedure could be very efficient for a control system. This procedure could be either a rather exact or one-to-one eigenvalue assignment to predefined locations, or a more general placement of the system's state space representation eigenvalues into convex sub-regions of the complex plane $P_{\mathbb{C}}$. The latter method is very appealing because it can be cast as an LMI convex optimization problem solvable by efficient algorithms.

$\mathcal{D}(\alpha, r, \vartheta)$ region

These regions may be vertical or horizontal strips, circles, parabolas or general conic sections on the complex plane. An LMI region used often in practice is the $\mathcal{D}(\alpha, r, \vartheta)$ performance-stability region of Fig. 3.4. This particular LMI region could define a useful design objective as it is the intersection of an α-stability vertical strip $\mathcal{D}_\alpha$ that provides a minimum decay rate α, a semi-circular region $\mathcal{D}_r$ imposing undamped natural frequency constraints and a triangular constraint region $\mathcal{D}_\vartheta$ that sets minimum damping on the closed loop eigenvalues. For any complex number $z = x + yj \in \mathbb{C}$ these regions are defined as:

$$\mathcal{D}_\alpha : \quad \mathcal{R}e\{z\} = x \leq -\alpha,\ \alpha > 0 \tag{3.11}$$

$$\mathcal{D}_r : \quad |z| \leq r,\ r > 0 \tag{3.12}$$

$$\mathcal{D}_\vartheta : \quad \tan\vartheta \cdot x \leq -|y|,\ 0 < \vartheta < \pi/2 \tag{3.13}$$

and

$$\mathcal{D}(\alpha, r, \vartheta) \triangleq \mathcal{D}_\alpha \cap \mathcal{D}_r \cap \mathcal{D}_\vartheta. \tag{3.14}$$

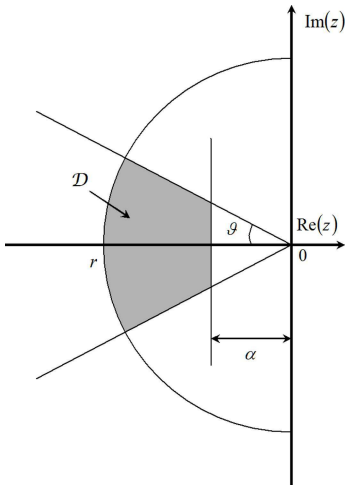

Figure 3.4: $\mathcal{D}$ performance-stability region.

3.1.2.2 D-Stability

In order to use the powerful machinery of LMI solvers to confine the eigenvalues of a plant inside a given region $\mathcal{D}$ of the complex plane $P_{\mathbb{C}}$, a formal definition of such a region is needed and it is given by the following statement [27]:

Definition 3.1. A subset $\mathcal{D}$ of the complex plane $P_{\mathbb{C}}$ is called an *LMI region* if there exists a symmetric matrix $\mathbf{\Lambda}$ with $\mathbf{\Lambda} = \mathbf{\Lambda}^T \in \mathbb{R}^{m\times m}$ and a matrix $\mathbf{M} \in \mathbb{R}^{m\times m}$ so that: LMI region

$$\mathcal{D} =: \{f_{\mathcal{D}}(z) < 0,\ z \in \mathbb{C}\} \tag{3.15}$$

with:

$$f_{\mathcal{D}}(z) = \mathbf{\Lambda} + z\mathbf{M} + \bar{z}\mathbf{M}^T. \tag{3.16}$$

□

Given the negative definitiveness of Eq. 3.15 the LMI regions are always convex and symmetric with respect to the negative real axis of $P_{\mathbb{C}}$ since $f_{\mathcal{D}}(\bar{z}) = \bar{f}_{\mathcal{D}}(z)$. In addition, more complex LMI regions may be constructed by simpler ones since they are in general invariant under set intersection[3]. This result was used for example in the previous section in order to construct the $\mathcal{D}(\alpha, r, \vartheta)$ performance-stability region of Fig. 3.4 and will be further exploited when it comes to the placement of the eigenvalues of a LTI system inside this region.

Consider the following LTI and finite dimensional unforced system with $x \in \mathbb{R}^{n\times 1}$ and $\mathbf{A} \in \mathbb{R}^{n\times n}$:

$$\dot{x} = \mathbf{A}x \tag{3.17}$$

[3]This means that the intersection $f_{\mathcal{D}_1} \cap f_{\mathcal{D}_2}$ of two LMI regions is also an LMI region with $f_{\mathcal{D}_1\cap\mathcal{D}_2} = \mathrm{Diag}(f_{\mathcal{D}_1}, f_{\mathcal{D}_2})$.

The necessary and sufficient condition for the plant to be *quadratically asymptotically stable* is the following well-known Lyapunov inequality condition:

$$\exists \mathbf{X} = \mathbf{X}^T > 0 : \quad \mathbf{A}\mathbf{X} + \mathbf{X}\mathbf{A}^T < 0. \tag{3.18}$$

The aforementioned condition may be extended for general *stable* subregions $\mathcal{D}$ of the complex plane (LMI regions) as in Definition 3.1; if the spectrum of $\mathbf{A}$ belongs to $\mathcal{D}$, then the system in Eq. 3.17 is called $\mathcal{D}$-stable. The following theorem gives necessary and sufficient conditions for $\mathcal{D}$-stability of such a system:

Stability condition for eigenvalue placement

Theorem 3.1. Consider the system of Eq. 3.17 and a convex LMI region $\mathcal{D}$, characterized by the matrices $\mathbf{\Lambda}, \mathbf{M}$ and described by the complex function $f_{\mathcal{D}}(z)$ as in Definition 3.1. Consider also the $m \times m$ block matrix $\mathbf{F}_{\mathcal{D}}(\mathbf{A}, \mathbf{X})$ with:

$$\begin{aligned} \mathbf{F}_{\mathcal{D}}(\mathbf{A}, \mathbf{X}) &= \mathbf{\Lambda} \otimes \mathbf{X} + \mathbf{M} \otimes (\mathbf{A}\mathbf{X}) + \mathbf{M}^T \otimes (\mathbf{A}\mathbf{X})^T \\ &= \left[\Lambda_{kl}\mathbf{X} + \mathrm{M}_{kl}\mathbf{A}\mathbf{X} + \mathrm{M}_{lk}(\mathbf{A}\mathbf{X})^T \right]_{1 \le k,l \le m} \end{aligned} \tag{3.19}$$

The system in Eq. 3.17 is then called $\mathcal{D}$-stable if and only if there exists a matrix $\mathbf{X} = \mathbf{X}^T > 0$ so that the following LMI condition holds:

$$\mathbf{F}_{\mathcal{D}}(\mathbf{A}, \mathbf{X}) < 0. \tag{3.20}$$

□

Proof. See [27], Appendix.

■

From the preceding analysis it is obvious that one could concatenate more than one LMI's of the form $\mathbf{F}_{\mathcal{D}_i}(\mathbf{A}, \mathbf{X}) < 0$ for each i'th LMI region; their intersection then forms the desired eigenvalue placement region of Eq. 3.14. This is exactly the power of the method since complex, performance-tailored LMI regions may be easily described in this way.

$\mathcal{D}(\alpha, r, \vartheta)$ stability conditions

The corresponding LMI conditions for each of the $\mathcal{D}(\alpha, r, \vartheta)$ subregions are given by the following expressions:

$$\mathcal{D}_\alpha : \quad \mathbf{A}\mathbf{X} + \mathbf{X}\mathbf{A}^T + 2\alpha\mathbf{X} < 0 \tag{3.21}$$

$$\mathcal{D}_r : \quad \begin{bmatrix} -r\mathbf{X} & \mathbf{A}\mathbf{X} \\ \mathbf{X}\mathbf{A}^T & -r\mathbf{X} \end{bmatrix} < 0. \tag{3.22}$$

$$\mathcal{D}_\vartheta : \quad \begin{bmatrix} \sin\vartheta \left(\mathbf{A}\mathbf{X} + \mathbf{X}\mathbf{A}^T\right) & \cos\vartheta \left(\mathbf{A}\mathbf{X} - \mathbf{X}\mathbf{A}^T\right) \\ \cos\vartheta \left(\mathbf{X}\mathbf{A}^T - \mathbf{A}\mathbf{X}\right) & \sin\vartheta \left(\mathbf{A}\mathbf{X} + \mathbf{X}\mathbf{A}^T\right) \end{bmatrix} < 0. \tag{3.23}$$

This concludes the analysis concerning the conditions for eigenvalue placement inside LMI regions. In the following section the synthesis equations for the calculation of an output feedback $\mathscr{H}_\infty$ controller with additional eigenvalue placement constraints[4] for the closed loop eigenvalues will be given.

[4]The regional constraints will be of the form as in Eqs. 3.21-3.23.

3.1.3 Controller Synthesis

Consider a finite dimensional LTI standard plant $\mathbb{P}(s)$ where $x \in \mathbb{R}^{n\times 1}$ is the state vector, $u \in \mathbb{R}^{n_u\times 1}$ the control vector, $y \in \mathbb{R}^{n_p\times 1}$ the measurement vector, $\zeta_\infty \in \mathbb{R}^{n_\zeta\times 1}$ a generalized performance vector and $w \in \mathbb{R}^{n_w\times 1}$ an external perturbation vector[5]:

$$\mathbb{P}: \quad \begin{aligned} \dot{x} &= \mathbf{A}x + \mathbf{B}_w w + \mathbf{B}_u u \\ \zeta_\infty &= \mathbf{C}_\zeta x + \mathbf{D}_{w\zeta} w + \mathbf{D}_{u\zeta} u \\ y &= \mathbf{C}_y x + \mathbf{D}_{wy} w + \mathbf{D}_{uy} u \end{aligned} \tag{3.24}$$

Standard plant P

Consider also an LMI $\mathcal{D}$-stability region $\mathcal{D}(\alpha, r, \vartheta)$ (see Fig. 3.4) and some $\mathscr{H}_\infty$ performance level $\gamma > 0$. The goal is to calculate an output feedback dynamic controller $K(s)$ in a standard l-LFT form (see Fig. 3.5) so that:

Synthesis constraints

- The eigenvalues of the closed loop system interconnection are placed inside the LMI region $\mathcal{D}(\alpha, r, \vartheta)$.
- The $\mathscr{H}_\infty$ performance level for the transfer function from the disturbance to the performance vector is satisfied; i.e. $\|T_{w\zeta_\infty}(s)\|_\infty < \gamma$ with $T_{w\zeta_\infty}(s) = \mathcal{F}_l(\mathbb{P}, K)$.

The output feedback controller $K(s)$ having as a task to achieve the aforementioned goals has the following standard form (with $x_k \in \mathbb{R}^{n_k\times 1}$ the controller state):

$$K: \quad \begin{aligned} \dot{x}_k &= \mathbf{A}_k x_k + \mathbf{B}_k y \\ u &= \mathbf{C}_k x_k + \mathbf{D}_k y. \end{aligned} \tag{3.25}$$

Feedback controller

The closed loop system transfer function $T_{w\zeta_\infty}(s)$ from the perturbation to the performance vector is written as:

$$T_{w\zeta_\infty}(s) \triangleq \mathbf{C}_{\text{cl}}(s\mathbb{I} - \mathbf{A}_{\text{cl}})^{-1}\mathbf{B}_{\text{cl}} + \mathbf{D}_{\text{cl}}. \tag{3.26}$$

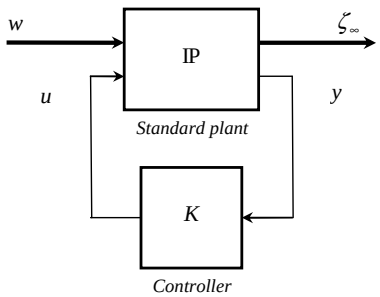

Figure 3.5: Standard l-LFT interconnection.

[5]The plant may be considered strictly proper ($\mathbf{D}_{uy} = 0$) without any loss of generality.

with:

$$\mathbf{A}_{\text{cl}} = \begin{bmatrix} \mathbf{A} + \mathbf{B}_u \mathbf{D}_k \mathbf{C}_y & \mathbf{B}_u \mathbf{C}_k \\ \mathbf{B}_k \mathbf{C}_y & \mathbf{A}_k \end{bmatrix} \tag{3.27}$$

$$\mathbf{B}_{\text{cl}} = \begin{bmatrix} \mathbf{B}_w + \mathbf{B}_u \mathbf{D}_k \mathbf{D}_{wy} \\ \mathbf{B}_k \mathbf{D}_{wy} \end{bmatrix} \tag{3.28}$$

$$\mathbf{C}_{\text{cl}} = \begin{bmatrix} \mathbf{C}_\zeta + \mathbf{D}_{u\zeta} \mathbf{D}_k \mathbf{C}_y & \mathbf{D}_{u\zeta} \mathbf{C}_k \end{bmatrix} \tag{3.29}$$

$$\mathbf{D}_{\text{cl}} = \mathbf{D}_{w\zeta} + \mathbf{D}_{u\zeta} \mathbf{D}_k \mathbf{D}_{wy}. \tag{3.30}$$

Before giving the formulas for controller synthesis, it should be outlined that these will involve the satisfaction of the BRL for the $\mathscr{H}_\infty$ part (with a Lyapunov matrix $\mathbf{X}_\infty$) and the eigenvalue placement LMI's of Eqs. 3.19-3.20 (with a Lyapunov matrix $\mathbf{X}$). However the problem is not tractable when considering two Lyapunov matrices so with some conservativeness it will be assumed that $\mathbf{X}_\infty = \mathbf{X}$. In addition, the BRL is not initially an LMI when substituting inside it the matrices of Eqs. 3.27-3.30 so a change of variables is needed (see [48]). The following theorem gives the final necessary and sufficient conditions for the problem:

Conditions for $\mathscr{H}_\infty$ control with eigenvalue placement constraints

Theorem 3.2. Let $\mathcal{D}$ be a desired LMI region of the complex plane $P_{\mathbb{C}}$ described by a characteristic function $f_{\mathcal{D}}(z)$ as in Eq. 3.16, with corresponding matrices $\mathbf{\Lambda}, \mathbf{M}$. There exist a Lyapunov matrix $\mathbf{X}$ and an output feedback controller $K(s) \triangleq \left[\begin{smallmatrix} \mathbf{A}_k & \mathbf{B}_k \\ \mathbf{C}_k & \mathbf{D}_k \end{smallmatrix}\right]$ that assure $\|T_{w\zeta_\infty}\|_\infty < \gamma$ and $\lambda(\mathbf{A}_{\text{cl}}) \in \mathcal{D}$ if and only if the following LMI's are satisfied:
Find $\mathbf{R} = \mathbf{R}^T, \mathbf{S} = \mathbf{S}^T \in \mathbb{R}^{n \times n}$ and matrices $\mathcal{A}_k, \mathcal{B}_k, \mathcal{C}_k, \mathbf{D}_k$ such that:

$$\begin{bmatrix} \mathbf{R} & \mathbb{I} \\ \mathbb{I} & \mathbf{S} \end{bmatrix} < 0 \tag{3.31}$$

$$\underset{1 \le k,l \le m}{} \left[\Lambda_{kl} \begin{bmatrix} \mathbf{R} & \mathbb{I} \\ \mathbb{I} & \mathbf{S} \end{bmatrix} + \mathrm{M}_{kl} \mathbf{\Phi} + \mathrm{M}_{lk} \mathbf{\Phi}^T \right] < 0 \tag{3.32}$$

$$\begin{bmatrix} \mathbf{\Psi}_{11} & \mathbf{\Psi}_{21}^T \\ \mathbf{\Psi}_{21} & \mathbf{\Psi}_{22} \end{bmatrix} < 0 \tag{3.33}$$

with the matrices $\mathbf{\Phi}, \mathbf{\Psi}_{11}, \mathbf{\Psi}_{21}, \mathbf{\Psi}_{22}$ being defined as:

$$\mathbf{\Phi} = \begin{bmatrix} \mathbf{AR} + \mathbf{B}_u \mathbf{C}_k & \mathbf{A} + \mathbf{B}_u \mathbf{D}_k \mathbf{C}_y \\ \mathcal{A}_k & \mathbf{SA} + \mathcal{B}_k \mathbf{C}_y \end{bmatrix} \tag{3.34}$$

$$\mathbf{\Psi}_{11} = \begin{bmatrix} \mathbf{AR} + (\mathbf{RA})^T + \mathbf{B}_u \mathcal{C}_k + (\mathbf{B}_u \mathcal{C}_k)^T & \mathbf{B}_w + \mathbf{B}_u \mathbf{D}_k \mathbf{D}_{wy} \\ (\mathbf{B}_w + \mathbf{B}_u \mathbf{D}_k \mathbf{D}_{wy})^T & -\gamma \mathbb{I} \end{bmatrix} \tag{3.35}$$

$$\mathbf{\Psi}_{21} = \begin{bmatrix} \mathcal{A}_k + (\mathbf{A} + \mathbf{B}_u \mathbf{D}_k \mathbf{C}_y)^T & \mathbf{SB}_w + \mathcal{B}_k \mathbf{D}_{wy} \\ \mathbf{C}_\zeta \mathbf{R} + \mathbf{D}_{u\zeta} \mathcal{C}_k & \mathbf{D}_{w\zeta} + \mathbf{D}_{u\zeta} \mathbf{D}_k \mathbf{D}_{wy} \end{bmatrix} \tag{3.36}$$

$$\mathbf{\Psi}_{22} = \begin{bmatrix} \mathbf{SA} + (\mathbf{SA})^T + \mathcal{B}_k \mathbf{C}_y + (\mathcal{B}_k \mathbf{C}_y)^T & (\mathbf{C}_\zeta + \mathbf{D}_{u\zeta} \mathbf{D}_k \mathbf{C}_y)^T \\ \mathbf{C}_\zeta + \mathbf{D}_{u\zeta} \mathbf{D}_k \mathbf{C}_y & -\gamma \mathbb{I} \end{bmatrix}. \tag{3.37}$$

□

Proof. See [27], pp. 365.

■

Controller reconstruction

Once the feasibility LMI's are solved obtaining $\mathbf{R}, \mathbf{S}, \mathcal{A}_k, \mathcal{B}_k, \mathcal{C}_k, \mathbf{D}_k$ and the minimal value of γ, the matrices $\mathbf{A}_k, \mathbf{B}_k, \mathbf{C}_k$ of a full-order controller (i.e. $n_k = n$) can be then computed[6]. To do this, first a full rank factorization $\mathbf{N}_1\mathbf{N}_2^T = \mathbb{I} - \mathbf{RS}$ (with $\mathbf{N}_1, \mathbf{N}_2$ being square and invertible) is performed using SVD. The matrices $\mathbf{N}_1, \mathbf{N}_2$ are in fact parts of the Lyapunov matrix $\mathbf{X}$ and its inverse partitioned as:

$$\mathbf{X} = \begin{bmatrix} \mathbf{R} & \mathbf{N}_1 \\ \mathbf{N}_1^T & \mathbf{U} \end{bmatrix} \tag{3.38}$$

$$\mathbf{X}^{-1} = \begin{bmatrix} \mathbf{S} & \mathbf{N}_2 \\ \mathbf{N}_2^T & \mathbf{V} \end{bmatrix}. \tag{3.39}$$

The controller matrices are finally calculated by inverting the transformations done to render the BRL convex[7]:

$$\mathcal{B}_k = \mathbf{N}_2\mathbf{B}_k + \mathbf{S}\mathbf{B}_u\mathbf{D}_k \tag{3.40}$$

$$\mathcal{C}_k = \mathbf{C}_k\mathbf{N}_1^T + \mathbf{D}_k\mathbf{C}_y\mathbf{R} \tag{3.41}$$

$$\mathcal{A}_k = \mathbf{N}_2\mathbf{A}_k\mathbf{N}_1^T + \mathbf{N}_2\mathbf{B}_k\mathbf{C}_y\mathbf{R} + \mathbf{S}\mathbf{B}_u\mathbf{C}_k\mathbf{N}_1 + \mathbf{S}(\mathbf{A} + \mathbf{B}_u\mathbf{D}_k\mathbf{C}_y)\mathbf{R}. \tag{3.42}$$

Obviously, if the eigenvalues of the system have to be confined inside a generic LMI region being the intersection of several basic LMI regions $\mathcal{D}_i$, as is the case with the $\mathcal{D}(\alpha, r, \vartheta)$ performance-stability region of Fig. 3.4, then several inequality conditions of the type as in Eq. 3.32 should be concatenated and satisfied simultaneously.

Technical Note: As far as practical implementation is concerned, one could either code the LMI feasibility conditions of Theorem 3.2 using available software for LMI solution (MATLAB® LMI Toolbox, YALMIP etc.) or use the available macro `hinfmix` of MATLAB® Robust Control Toolbox which performs multi-objective $\mathscr{H}_2/\mathscr{H}_\infty$ synthesis with eigenvalue placement constraints. This macro gives the dynamic controller $K(s)$ satisfying all the constraints as well as the minimum γ attained and the feasibility matrices $\mathbf{R}, \mathbf{S}$ of Theorem 3.2.
The macro `hinfmix` takes the argument `'region'` that is consisted in fact of the matrices $\mathbf{\Lambda}, \mathbf{M}$ characterizing the LMI region $\mathcal{D}$ used for the eigenvalue placement. The argument `'region'` is obtained from an interactive dialog with the user by the macro `lmireg` of the same toolbox. A predefined inventory with various LMI regions (horizontal and vertical strips, disks, conic sections etc.) is available by default.

[6] More precisely the order n_k is equal to rank($\mathbf{RS} - \mathbb{I}$), with $\mathbf{R}, \mathbf{S}$ given by Theorem 3.2.
[7] The final implemented controller is given then by Eq. 3.25.

3.2 Compensator Estimator-Controller Form

In this section some results will be presented on the subject of converting a generic compensator $K(s)$ into an equivalent observer/state feedback controller form. A very good treatment of the subject can be found in [4] with most of the material drawn from the original work found in [20, 21].

3.2.1 Motivation

The conversion of a generic compensator $K(s)$ to an observer/state feedback controller form may be useful for two reasons. The first has to do with the advantage of observer/state feedback controllers to preserve the same state representation as the plant for which they have been computed, since the controller states can be viewed as estimates of the plant's states. The second reason is relevant with gain scheduling; if the compensator's parameters are to be changed/updated, it is better to update only the two matrices $\mathbf{K}_{\mathrm{c}}, \mathbf{K}_{\mathrm{o}}$ of the observer/state feedback form of the compensator instead of updating the compensator matrices $\mathbf{A}_k, \mathbf{B}_k, \mathbf{C}_k, \mathbf{D}_k$.

The material of this section will be used in conjunction with the analysis of Section 3.1, where dynamic compensators with eigenvalue placement constraints are designed, in order to conceive gain-scheduled control laws based on the observer/state feedback controller interpolation technique of Chapter 5.

3.2.2 Controller Transformation

The general idea is based on the fact that an output feedback dynamic compensator $K(s)$ of the form (with $x_k \in \mathbb{R}^{n_k \times 1}$ being the compensator state vector and $n_k \geq n$):

$$K: \quad \begin{aligned} \dot{x}_k &= \mathbf{A}_k x_k + \mathbf{B}_k y \\ u &= \mathbf{C}_k x_k + \mathbf{D}_k y. \end{aligned} \tag{3.43}$$

may be transformed to an equivalent observer/state feedback controller being of the same order as the plant for which it has been computed (order n) plus the famous Youla parameter $Q(s)$ that is an always stable system of order $n_k - n$.

Discussion on the Youla parameter

In order to avoid having an additional dynamical system $Q(s)$ for which interpolation should be also used when coming to gain scheduling, the compensators designed must be forced to have *the same order* as the plant. In this case, after the transformation that will be detailed in the following lines, the Youla parameter becomes only a static gain:

$$Q(s) \equiv \mathbf{D}_k. \tag{3.44}$$

Furthermore, if the compensators designed are restricted to be strictly proper, then the Youla parameter is zero and the compensator $K(s)$ may be represented by a standard Kalman observer plus a state feedback gain (see Fig. 3.6).

The conversion formulas will now be given according to [4]. Consider without loss of generality a finite dimensional strictly proper LTI system $G(s)$ with the following state space representation (with $x \in \mathbb{R}^{n\times 1}$ the state vector, $u \in \mathbb{R}^{n_u\times 1}$ the control vector and $y \in \mathbb{R}^{n_y\times 1}$ the measurement vector):

$$G: \quad \begin{aligned} \dot{x} &= \mathbf{A}x + \mathbf{B}u \\ y &= \mathbf{C}x. \end{aligned} \tag{3.45}$$

Consider also a LTI dynamic output feedback compensator as in Eq. 3.43[8] that stabilizes the plant and may also provide additional useful properties such as robustness to external perturbations, eigenvalue placement etc.

Conversion procedure

The idea here is to transform the dynamic controller $K(s)$ in such a way so that it would be a Kalman observer of a linear transformation of the plant state x or:

$$x_k = \mathbf{T}\hat{x}. \tag{3.46}$$

A Kalman observer of the system's state plus the state feedback controller are written as:

$$\begin{aligned} \dot{\hat{x}} &= \mathbf{A}\hat{x} + \mathbf{B}u + \mathbf{K}_\mathrm{o}(y - \mathbf{C}\hat{x}) \\ u &= \mathbf{K}_\mathrm{c}\hat{x}. \end{aligned} \tag{3.47}$$

If the state feedback controller equation is substituted to the observer one then the following dynamic controller is obtained:

$$\begin{aligned} \dot{\hat{x}} &= (\mathbf{A} + \mathbf{B}\mathbf{K}_\mathrm{c} - \mathbf{K}_\mathrm{o}\mathbf{C})\hat{x} + \mathbf{K}_\mathrm{o}y \\ u &= \mathbf{K}_\mathrm{c}\hat{x}. \end{aligned} \tag{3.48}$$

Now if the state transformation of Eq. 3.46 is performed to Eq. 3.48, then the following compensator form is calculated:

$$\begin{aligned} \dot{x}_k &= \mathbf{T}(\mathbf{A} + \mathbf{B}\mathbf{K}_\mathrm{c} - \mathbf{K}_\mathrm{o}\mathbf{C})\mathbf{T}^{-1}x_k + \mathbf{T}\mathbf{K}_\mathrm{o}y \\ u &= \mathbf{K}_\mathrm{c}\mathbf{T}^{-1}x_k. \end{aligned} \tag{3.49}$$

Finally, by performing an one to one identification of the controller matrices of Eq. 3.49 using Eq. 3.47, the following conditions are found:

$$\mathbf{A}_k\mathbf{T} - \mathbf{T}\mathbf{A} - \mathbf{T}\mathbf{B}\mathbf{C}_k\mathbf{T} + \mathbf{B}_k\mathbf{C} = 0 \tag{3.50}$$

and:

$$\mathbf{K}_\mathrm{o} = \mathbf{T}^{-1}\mathbf{B}_k \tag{3.51}$$

$$\mathbf{K}_\mathrm{c} = \mathbf{C}_k\mathbf{T}. \tag{3.52}$$

Equation 3.50 is a generalized non-symmetric rectangular Riccati equation that can be solved using the following technical note. After it has been solved, the observer/controller matrices of Eqs. 3.51-3.52 may be finally computed.

[8] The compensator $K(s)$ is considered strictly proper ($\mathbf{D}_k = 0$).

Technical Note: To solve the Riccati equation [9] (Eq. 3.50), it suffices to observe that it may be written as:

$$\begin{bmatrix} -\mathbf{T} & \mathbb{I} \end{bmatrix} \begin{bmatrix} \mathbf{A} & \mathbf{B}\mathbf{C}_k \\ \mathbf{B}_k\mathbf{C} & \mathbf{A}_k \end{bmatrix} \begin{bmatrix} \mathbb{I} \\ \mathbf{T} \end{bmatrix} = 0. \tag{3.53}$$

The matrix in the middle of Eq. 3.53 is nothing else than the closed loop matrix of the system $\mathbf{A}_{\text{cl}}$ (see Eq. 3.27 with $\mathbf{B}_u = \mathbf{B}, \mathbf{C}_y = \mathbf{C}$ and $\mathbf{D}_k = 0$). Use then eigenvector decomposition in order to find a matrix $\mathbf{U}$ and a matrix $\mathbf{\Lambda}$ so that:

$$\mathbf{U}^{-1}\mathbf{A}_{\text{cl}}\mathbf{U} = \mathbf{\Lambda}. \tag{3.54}$$

Then compute the solution to the generalized non-symmetric rectangular Riccati equation of Eq. 3.50 as:

$$\mathbf{T} = \mathbf{U}_{21}\mathbf{U}_{11}^{-1} \tag{3.55}$$

where the matrix $\mathbf{U}$ is partitioned as $\mathbf{U} = \begin{bmatrix} \mathbf{U}_{11} & \mathbf{U}_{12} \\ \mathbf{U}_{21} & \mathbf{U}_{22} \end{bmatrix}$.

Eigenvalue ordering

Now if the eigenvalues of the closed loop system *are not repeated*, then the columns of $\mathbf{U}$ are simply the eigenvectors of the closed loop system matrix $\mathbf{A}_{\text{cl}}$ and $\mathbf{\Lambda}$ is a diagonal matrix whose elements are the eigenvalues of $\mathbf{A}_{\text{cl}}$. The solutions of the Riccati equations are not unique since each solution correspond to a different ordering of the columns of $\mathbf{U}$. In general, the eigenvectors should be ordered in such a way that the first n ones correspond to the closed loop controller eigenvalues whereas the rest to the n estimator eigenvalues. This ordering should be done according to the rapidity of the eigenvalues and is not always trivial (for further discussion see [21]). The possible orderings are in fact the combinations of n eigenvalues out of totally $2n$ or $\binom{2n}{n}$ and can be as high as 20 for a third order compensator.

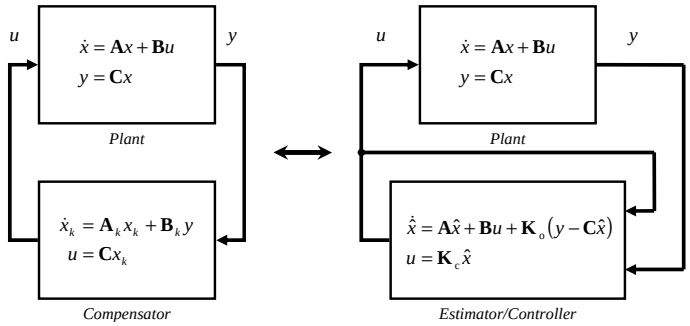

Figure 3.6: Compensator and estimator/controller equivalence.

[9] For alternative methods to solve the Riccati equation see [20], pp. 1576 and references therein.

3.3 $\mathscr{H}_\infty$ Loop Shaping

In this section, an alternative method to the classic $\mathscr{H}_\infty$ formulation for the design of robust output feedback controllers of Section 3.1 will be presented. This method is based on the famous *loop shaping* approach for the design of MIMO output feedback controllers first introduced in [98].

In Section 3.3.1 the principal ideas motivating the method are presented whereas in Section 3.3.2 the method itself is outlined. The solution to the problem of designing full order controllers, satisfying the analysis of Sections 3.3.1, 3.3.2 using the Riccati and LMI-based formulation, is presented in 3.3.3. Finally in Section 3.3.4 the problem of designing a static instead of a full order controller is described.

3.3.1 Motivation

Standard $\mathscr{H}_\infty$ control vs. LSDP

The methodology of designing a classic $\mathscr{H}_\infty$ robust output feedback controller $K(s)$ for a LTI system $G(s)$ is mainly based on shaping the singular values of certain transfer functions of the closed loop via the use of weighting filters. These closed loop transfer functions are defined using an input vector w representing external disturbances and/or reference signals and an output vector ζ_∞ representing critical signals on the closed loop system needing particular treatment as for example error and/or control signals (see Fig. 3.5). Then a stabilizing controller is computed, ensuring that the $\mathscr{H}_\infty$ norm of the transfer function $T_{w\zeta_\infty}(s) = \mathcal{F}_l(\mathbb{P}, K)$ from w to ζ_∞ is minimized. Additional constraints (such as closed loop eigenvalue placement ones) could be subsequently added as in Section 3.1.

A major disadvantage of this method is that the choice of the weighting functions used is either highly empirical or involves a great number of trial and error experiments until a good compromise between performance and robustness is found. At the end, one cannot be sure that the best choice of filters has been done and as a result, it cannot be argued that the controller computed is the optimal one (even though it is optimal (or sub-optimal) for the selected filters).

An alternative to this method is the so-called *loop shaping design procedure* (LSDP) first introduced in [98]. It is based on the fact that performance and robustness optimization could be separated in two phases (retaining always a trade-off between the two) and therefore obtain more flexibility in controller design. This procedure uses this time the *open loop* singular values $\sigma(GK)$ over specified frequency ranges in order to characterize the closed loop performance and robustness of the plant instead of using directly various weighted *closed loop* transfer functions as with standard $\mathscr{H}_\infty$ control.

This in fact is in accordance with the classic SISO control practice where controllers are designed in order to achieve high/low open loop gain at low/high frequencies for good performance/robustness and a correct roll off rate at the gain crossover frequency to maintain stability avoiding excessive phase lag.

Generalized feedback scheme

To prove that in fact it is possible to describe *closed loop* performance and robustness requirements by the use of *open loop* information, consider the following generalized feedback interconnection scheme where d, n may model various disturbances, sensor noises or reference signals acting on the plant G, whereas y, u are the inputs/outputs to the controller K.

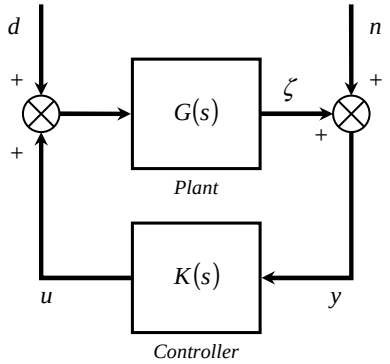

Figure 3.7: Generalized feedback interconnection.

The reason for which this feedback structure is chosen is twofold. First it incorporates all possible external signals acting on G in a general manner. Second it permits to define an uncertain system G_Δ with additive perturbations to its coprime factors in a straightforward way as it will be presented at the end of this section. The controller K is then computed to stabilize the plant G in the face of such uncertainties in the context of the LSDP. As an extension to this stabilization property, this feedback structure permits also the introduction of another significant system notion: the *gap metric*. The interconnection of the gap metric and the robust stabilization of an uncertain system G_Δ using a controller K is very important as it will be shown in Section 3.4 and it will be used for the development of gain-scheduled control laws in Chapter 6.

The analysis presented further down will show that many performance and requirements for a closed loop system may be incorporated using the feedback scheme shown in Fig. 3.7. The transfer functions considered are the ones from the external disturbances n, d to the controller output/inputs y, u. After simple matrix manipulation one gets:

$$\begin{bmatrix} u \\ y \end{bmatrix} = \begin{bmatrix} KS & T' \\ S & SG \end{bmatrix} \begin{bmatrix} n \\ d \end{bmatrix}. \tag{3.56}$$

In the previous equation S is called the *output sensitivity matrix* and T' the *input complementary sensitivity matrix* defined as:

$$S \triangleq (\mathbb{I} - GK)^{-1} \tag{3.57}$$

$$T' \triangleq K(\mathbb{I} - GK)^{-1}G = KSG. \tag{3.58}$$

A very good control strategy, following a classic $\mathscr{H}_\infty$ formulation, is in fact to design a stabilizing controller K in such a way that the effect of the input/output disturbances d, n on the open loop plant G is also minimized over all frequencies. This means that K is designed to satisfy:

$$\left\| \begin{bmatrix} KS & T' \\ S & SG \end{bmatrix} \right\|_\infty \equiv \left\| \begin{bmatrix} SG & T \\ S' & KS \end{bmatrix} \right\|_\infty < \gamma, \quad \gamma > 0 \tag{3.59}$$

with S' being the *input sensitivity matrix* and T the *output complementary sensitivity matrix* defined as[10]:

$$S' \triangleq (\mathbb{I} - KG)^{-1} \tag{3.60}$$

$$T \triangleq GK(\mathbb{I} - GK)^{-1} = GKS. \tag{3.61}$$

From *open* to *closed*-loop objectives

The minimization of the $\mathscr{H}_\infty$-norm of each one of the six closed loop transfer functions-objectives S, S', T, T', SG, KS of Eq. 3.59 over all frequencies is not generally possible because there is always a conflict between them due to the fact that for example $S + T = \mathbb{I}$. However this minimization could be performed for different zones of frequencies and also considering *open loop* instead of these *closed loop* objectives.

Take for instance the $\mathscr{H}_\infty$-norm of the output sensitivity matrix S which can be studied by studying its maximum singular values $\overline{\sigma}(S)$ for all frequencies. For frequencies where the minimum singular values of the open loop transfer function are big (i.e. $\underline{\sigma}(GK) \gg 1$), then the following approximation holds (see [155], pp. 131-133, 486 or [96], pp. 102):

$$\overline{\sigma}(S) = \overline{\sigma}\big((\mathbb{I} - GK)^{-1}\big) \simeq \frac{1}{\underline{\sigma}(GK)} \tag{3.62}$$

The sensitivity function gives the influence of output disturbances n to the plant output y. If these disturbances n are reference signals (typically low frequency ones) then $\|S\|_\infty$ should be minimized for low frequencies in order to ensure good reference tracking and hence from Eq. 3.62, $\underline{\sigma}(GK)$ should be maximized for a *low* frequency band $\omega < \omega_l$.

In conflict with the above requirement, suppose the output disturbance n is a high frequency noise. The complementary sensitivity function $T = GKS$ gives the *closed loop* noise influence on the plant output ζ. The maximum singular values of T can be approximated for some frequencies where the maximum of the *open loop* singular values are small ($\overline{\sigma}(GK) \ll 1$) with:

$$\overline{\sigma}(T) = \overline{\sigma}\big(GK(\mathbb{I} - GK)^{-1}\big) \simeq \overline{\sigma}(GK). \tag{3.63}$$

In this case (and given that n appears in high frequencies) $\overline{\sigma}(GK)$ should be minimized at a *high* frequency band $\omega > \omega_h$. As a final remark it could be added that the frequency zone (ω_l, ω_h), defining the *roll-off* rate, cannot be made very small since this could lead to excessive phase lag and hence instability[11].

[10] The classic relations $S + T = \mathbb{I}$ and $S' + T' = \mathbb{I}$ always hold.

[11] A theoretical maximum is -40db/dec but in practice a 20db/dec rate is preferred.

On loop shaping

The two aforementioned closed loop objectives (reference signal tracking, output measurement noise rejection) are typically *performance* and *robustness* ones and can be adjusted by making the minimum/maximum *open loop* system singular values big/small at low/high frequencies ($\omega < \omega_l, \omega > \omega_h$) respectively while retaining a roll of rate of around $20db/dec$ for intermediate frequencies. Typically this leads to a singular value shaping as in Fig. 3.8[12].

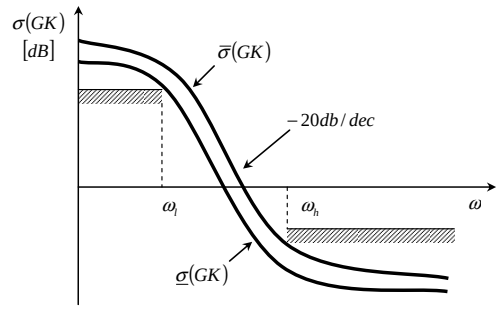

Figure 3.8: Shaping of the open loop singular values.

In the context of the LSDP (see Section 3.3.2), these *open loop* singular values could be 'shaped' using appropriate pre/post filters W_1, W_2 before and after the system G so that the shaped open loop plant's $G_s = W_2 G W_1$ singular values have a desired shape (see Fig. 3.8). However, this shaping is done *without regarding the plant's phase* (except for a rough demand on the roll-off rate) and hence loop stability. The solution to this problem is addressed by adding an additional controller acting on G_s in such a way that guarantees loop stability. In the LSDP procedure, this controller is of a special type: it stabilizes but additionally it renders the loop robust over left unstructured NCF uncertainties.

NCF robust stab/tion

In the remainder of this section, this problem of robust stabilization over left unstructured NCF uncertainties is posed. Its solution is presented in Section 3.3.3 using both the standard Glover/Doyle and the equivalent LMI formulations. In addition further down it will be shown that the solution to this four-block shaping problem of Eq. 3.59 detailed before, and which has a standard $\mathscr{H}_\infty$ formulation, is equivalent to this robust stabilization problem.

The question however arising is why consider such a specific type of uncertainties. It has been argued in [143, 144] that this way of representing process uncertainty is very attractive since no particular information in its form in demanded and hence general perturbed plants G_Δ that are situated 'around' a nominal plant G could be considered. This could be of use for example for linearized plants of a nonlinear system being computed on equilibrium points close enough to a reference equilibrium point; these linearized plants could be considered as perturbed plants G_Δ over the reference plant G.

[12] Additionally one could also treat the closed loop objectives SG, KS that boil down to specifications on the controller's minimum/maximum singular values $\underline{\sigma}(K), \overline{\sigma}(K)$ for low/high frequencies (performance/robustness specifications respectively) by further adjusting K.

NCF perturbed system

Start by considering the left NCF representation of a nominal plant $G(s)$ as (with $\tilde{N}\tilde{N}^* + \tilde{M}\tilde{M}^* = \mathbb{I}$)[13]:

$$G \triangleq \tilde{M}^{-1}\tilde{N}. \tag{3.64}$$

A perturbed plant G_Δ with the perturbations acting on its left NCF's is considered as (see Fig. 3.9)[14]:

$$G_\Delta = (\tilde{M} + \Delta_M)^{-1}(\tilde{N} + \Delta_N) \tag{3.65}$$

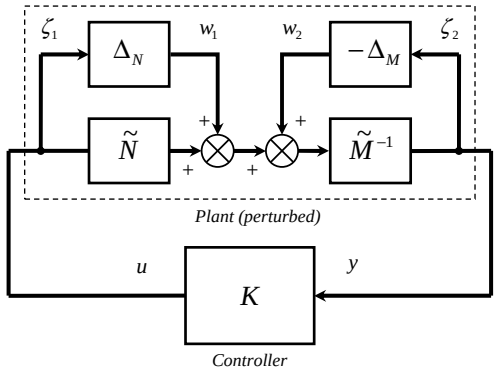

Figure 3.9: NCF perturbed plant.

If $w = w_1 + w_2$ is the external perturbation, $\zeta_\infty = [\zeta_1\ \zeta_2]^T = [u\ y]^T$ is the performance vector and the uncertainty is regrouped as $\Delta = [\Delta_N\ -\Delta_M]$, then the perturbed plant can be written as the upper linear fractional transformation (u-LFT) of the standard plant $\mathbb{P} = \left[\begin{smallmatrix} P_{11} & P_{12} \\ P_{21} & P_{22} \end{smallmatrix}\right]$ (corresponding to the nominal plant G) and the unstructured uncertainty Δ as:

$$\begin{aligned} G_\Delta &= \mathcal{F}_U(\mathbb{P}, \Delta) \\ &\triangleq P_{22} + P_{21}\Delta(\mathbb{I} - P_{11}\Delta)^{-1}P_{12}. \end{aligned} \tag{3.66}$$

where the following standard I/O signal expression:

$$\begin{bmatrix} \zeta_\infty \\ y \end{bmatrix} = \mathbb{P} \begin{bmatrix} w \\ u \end{bmatrix} \tag{3.67}$$

defines $\mathbb{P}$ as:

$$\mathbb{P} = \begin{bmatrix} 0 & \mathbb{I} \\ \tilde{M}^{-1} & G \\ \tilde{M}^{-1} & G \end{bmatrix}. \tag{3.68}$$

[13] In the context of the LSDP this open loop plant will be in fact an already shaped one $G_s = W_2 G W_1$.

[14] The perturbations considered are unstructured & unknown but stable & bounded transfer functions with $\left\|[\Delta_M\ \Delta_N]\right\|_\infty < \epsilon$ and $\epsilon > 0$.

The NCF robust stab/tion problem

The NCF *robust stabilization problem* of G (equivalently G_s in the LSDP) with a controller K is taken for their l-LFT $\mathcal{F}_L(\mathbb{P}, K)$ with:

$$\mathcal{F}_L(\mathbb{P}, K) \equiv \begin{bmatrix} KS\tilde{M}^{-1} \\ S\tilde{M}^{-1} \end{bmatrix}. \tag{3.69}$$

A formal definition of the NCF optimal robust stabilization problem is given in the following theorem [96, 97]:[15]

Theorem 3.3. Consider a plant G and stable norm-bounded left NCF uncertainties $\Delta = [\Delta_N \ -\Delta_M]$ with $\|\Delta\|_\infty < \epsilon$ and $\epsilon > 0$. A robust controller K stabilizes the perturbed plant $G_\Delta = \mathcal{F}_U(\mathbb{P}, \Delta)$ for all such Δ with $\mathbb{P}$ being the related to G standard plant if and only if:

a. K stabilizes G.

b. $\|\mathcal{F}_L(\mathbb{P}, K)\|_\infty = \left\| \begin{bmatrix} K(\mathbb{I} - GK)^{-1}\tilde{M}^{-1} \\ (\mathbb{I} - GK)^{-1}\tilde{M}^{-1} \end{bmatrix} \right\|_\infty \leq \epsilon^{-1}$.

□

Proof. See [96], pp. 33-36.

■

From *two* to *four*-block problem

The above *two-block* robust optimization problem is proven immediately to be equivalent to the initial *four-block* disturbance rejection problem since the factorization of G is normalized and:

$$\begin{bmatrix} \mathbb{I} & G \end{bmatrix} = \tilde{M}^{-1} \begin{bmatrix} \tilde{M} & \tilde{N} \end{bmatrix}. \tag{3.70}$$

So finally Eqs. 3.59, 3.69 are equivalent:

$$\begin{aligned} \left\| \begin{bmatrix} K(\mathbb{I} - GK)^{-1} & K(\mathbb{I} - GK)^{-1}G \\ (\mathbb{I} - GK)^{-1} & (\mathbb{I} - GK)^{-1}G \end{bmatrix} \right\|_\infty &\equiv \left\| \begin{bmatrix} K(\mathbb{I} - GK)^{-1}\tilde{M}^{-1} \\ (\mathbb{I} - GK)^{-1}\tilde{M}^{-1} \end{bmatrix} \right\|_\infty \\ \Leftrightarrow \left\| \begin{bmatrix} K \\ \mathbb{I} \end{bmatrix} (\mathbb{I} - GK)^{-1} \begin{bmatrix} \mathbb{I} & G \end{bmatrix} \right\|_\infty &\equiv \left\| \begin{bmatrix} K \\ \mathbb{I} \end{bmatrix} (\mathbb{I} - GK)^{-1}\tilde{M}^{-1} \right\|_\infty. \end{aligned} \tag{3.71}$$

The motivation for the use of robust stabilizing $\mathscr{H}_\infty$ controllers is now clear: since the feedback loop could obtain some good initial performance and maybe robustness properties by the use for example of some pre-compensators shaping its open loop singular values, such an $\mathscr{H}_\infty$ stabilizing controller could be subsequently added in the loop rendering it also robust over generalized unstructured coprime factor uncertainties. This procedure outlined here will be presented in detail in the following section.

[15] It is of course attempted to maximize this robustness margin ϵ to an optimum value $\epsilon_{\max}$.

3.3.2 The Loop Shaping Design Procedure (LSDP)

The *loop shaping design procedure* (LSDP) of McFarlane & Glover presented in detail in [97], [96] - Ch. 6, [155] - Ch. 18, [93] - Ch. 12 will be outlined in the first part of this section. Some results concerning this method will equally be presented in the second part[16]. The LSDP can be divided in three distinct steps and is visualized in Figs. 3.10a, 3.10b. These steps are:

The LSDP

Step 1 - Loop Shaping. The initial open loop plant $G(s)$ is augmented using pre/post compensators W_1, W_2 in order to shape the singular values $\sigma(G_\mathrm{s})$ of the new augmented *open loop* plant $G_\mathrm{s} = W_2 G W_1$, following the analysis of the previous section (see Fig. 3.8). Typically the designer chooses W_1 as a low pass filter in order to have a sufficiently small loop gain in high frequencies ($\omega > \omega_h$) and W_2 in order to assure a good tracking performance with high loop gain in low frequencies ($\omega < \omega_l$). In addition the compensators should also be chosen in such a way so as to avoid excessive roll-off rates (and hence instability) in intermediate frequencies (typically around the gain crossover frequency ω_g); a good value being about $-20dB/dec$[17].

Step 2 - Controller Calculation. The maximum robustness margin ϵ_max achieved by a robust stabilizing controller K_∞, designed for the open loop system G_s, can be calculated before actually K_∞ is computed (see Section 3.3.3). This maximum stability margin ϵ_max is also a measure of the success of the loop shaping performed in *Step 1*. If $\epsilon_\mathrm{max} \ll 1$ then there is an incompatibility between the chosen loop shape, the shaped plant's phase and robust closed loop stability; thus W_1, W_2 should be readjusted. If ϵ_max is satisfactory (typically around 0.3), then select a sub-optimal $\epsilon < \epsilon_\mathrm{max}$ and calculate the $\mathscr{H}_\infty$ controller K_∞ that robustly stabilizes the loop.

Step 3 - Controller Implementation. The final controller $K_\mathrm{s} = W_1 K_\infty W_2$ being the series interconnection of the pre/post compensators and the robust controller may now be implemented. The order of K_s is equal to the order of the plant n plus the sum of the orders of the pre/post compensators $n_w = n_{w_1} + n_{w_2}$. As a result, the order n_s of the final controller is $n + 2n_w$, fact that could be conservative for implementation. To solve this problem, model reduction techniques could be applied on K_∞ while using compensators W_1, W_2 of the simplest possible structure. Another solution could be the design of a reduced order or even a static robust controller K_∞ from the beginning, a problem which is in general difficult to solve[18].

[16] This method gives a solid alternative to classic $\mathscr{H}_\infty$ control strategy. It has been applied to a big number of study cases (see Section 5.2 for a comprehensive review).

[17] Note that the compensators may also be unstable and/or having poles/zeros on the imaginary axis without this fact posing any problems since they are on the feedback loop in contrast to the classic $\mathscr{H}_\infty$ practice.

[18] In the context of gain-scheduled control where reduced order controllers are of particular interest, a solution to this problem is given in Section 3.3.4.

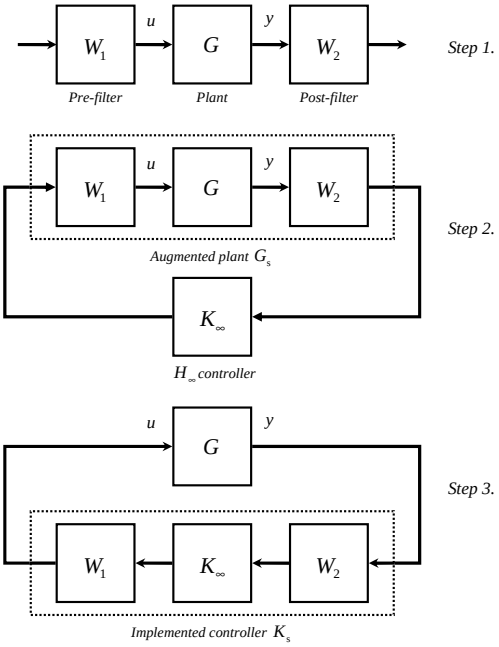

(a) *Block diagram form*

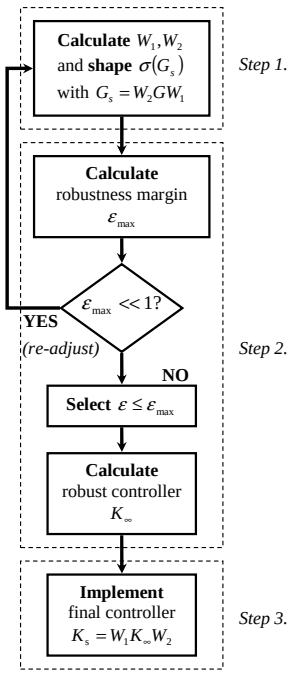

(b) *Algorithm form*

Figure 3.10: The loop shaping design procedure (LSDP).

The robust controller $K_\mathrm{s} = W_1 K_\infty W_2$ calculated using the LSDP will try to stabilize the plant while also rendering it robust to coprime factor uncertainties. However it may be possible that it will degrade the singular value shape of the initial open loop $G_s = W_2 G W_1$ adjusted with the pre-post compensators. The following analysis shows that it is in fact possible to compute maximum limits for this degradation that depend not on the controller K_∞ but only on the singular value shape of the initial open loop and also on the robustness margin ϵ that may be achieved by K_∞. Given however that this robustness margin depends by its turn *only* on W_1, W_2 (and hence on G_s), it follows that the degradation is dependent only on the initial loop shape.

Degradation of the initial loop shape

To compute this degradation it is imperative to compare the initial loop shape of $G_s = W_2 G W_1$ with the final ones $W_1 K_\infty W_2 G = K_\mathrm{s} G$ at the plant input and $G W_1 K_\infty W_2 = G K_\mathrm{s}$ at the plant output. For low (respectively high) frequencies the minimum (respectively maximum) singular values of the initial and final open loop shapes are compared.
For *low frequencies* the following relations hold[19]:

$$\textit{Plant output:} \qquad \underline{\sigma}(GK_\mathrm{s}) \geq \frac{\underline{\sigma}(G_\mathrm{s})\underline{\sigma}(K_\infty)}{c(W_2)} \tag{3.72}$$

$$\textit{Plant input:} \qquad \underline{\sigma}(K_\mathrm{s}G) \geq \frac{\underline{\sigma}(G_\mathrm{s})\underline{\sigma}(K_\infty)}{c(W_1)} \tag{3.73}$$

whereas for *high frequencies*:

$$\textit{Plant output:} \qquad \overline{\sigma}(GK_\mathrm{s}) \leq \overline{\sigma}(G_\mathrm{s})\overline{\sigma}(K_\infty)c(W_2) \tag{3.74}$$

$$\textit{Plant input:} \qquad \overline{\sigma}(K_\mathrm{s}G) \leq \overline{\sigma}(G_\mathrm{s})\overline{\sigma}(K_\infty)c(W_1). \tag{3.75}$$

The only obstacle to find a lower (respectively upper) bound for the low (respectively high) frequency loop shape deterioration at the input/output of the plant is to obtain bounds on the minimum (respectively maximum) singular values of the controller K_∞. This bound is obtained in [96], pp. 110-116:

$$\underline{\sigma}(K_\infty) \geq \frac{\underline{\sigma}(G_\mathrm{s}) + \sqrt{\gamma^2 - 1}}{1 + \underline{\sigma}(G_\mathrm{s})\sqrt{\gamma^2 - 1}} \quad \text{for } \forall\omega \text{ where} \quad \underline{\sigma}(G_\mathrm{s}) > \sqrt{\gamma^2 - 1} \tag{3.76}$$

$$\overline{\sigma}(K_\infty) \leq \frac{\overline{\sigma}(G_\mathrm{s}) - \sqrt{\gamma^2 - 1}}{1 - \overline{\sigma}(G_\mathrm{s})\sqrt{\gamma^2 - 1}} \quad \text{for } \forall\omega \text{ where} \quad \overline{\sigma}(G_\mathrm{s}) < \frac{1}{\sqrt{\gamma^2 - 1}}. \tag{3.77}$$

In addition these two bounds $\underline{\sigma}(K_\infty), \overline{\sigma}(K_\infty)$ tend asymptotically to $\dfrac{1}{\sqrt{\gamma^2 - 1}}$ and to $\sqrt{\gamma^2 - 1}$ respectively if the values of $\underline{\sigma}(G_\mathrm{s})$ and $\overline{\sigma}(G_\mathrm{s})$ are much greater than $\sqrt{\gamma^2 - 1}$ and much smaller than $\dfrac{1}{\sqrt{\gamma^2 - 1}}$ respectively, with $\gamma \triangleq \epsilon^{-1}$.

[19] $c(G)$ denotes the frequency dependent condition number of G with $c(G) = \dfrac{\overline{\sigma}(G)}{\underline{\sigma}(G)}$.

In addition to the previous results linking the initial loop shape specified by the use of the pre/post compensators and the final loop shape when the $\mathscr{H}_\infty$ controller has been added there are also results concerning the behavior of the closed loop performance & robustness objectives $S, SG, K_\mathrm{s}S, K_\mathrm{s}SG$. Briefly it can be said that bounds on these closed loop objectives can also be computed as a function of γ, G, W_1 and W_2 only[20].

In this section the standard McFarlane & Glover loop shaping design procedure (LSDP) has been detailed and some theoretical results justifying this procedure presented. In the context of gain-scheduled control considered in this work, this procedure will be used for the design of LTI controllers for LTI approximations of nonlinear systems around a set of equilibrium points in Chapter 6.

3.3.3 Full Order Case

In this section the solution to the sub-optimal robust stabilization problem of Theorem 3.3 linked to the LSDP of Section 3.3.2 will be given. For completeness, both the solution based on the classic Glover & Doyle formulation [53] and an LMI formulation will be detailed in the following two subsections.

Briefly the problem is to find a dynamic output feedback stabilizing controller K_∞ to the already shaped open loop plant $G_\mathrm{s} = W_2GW_1$ of Fig. 3.10a[21] that also satisfies the requirement:

$$\left\| \begin{bmatrix} K_\infty \\ \mathbb{I} \end{bmatrix} (\mathbb{I} - G_\mathrm{s}K_\infty)^{-1}\tilde{M}^{-1} \right\|_\infty \leq \gamma, \quad \gamma > 0. \tag{3.78}$$

Robustness margin

It is clear that if $\epsilon_{\max}$ is the maximum robustness margin that can be achieved, an $\epsilon \lesssim \epsilon_{\max}$ is chosen in order to construct the robust controller with $\gamma = 1/\epsilon$ and typically $2 < \gamma < 10$. The controller K_∞ will robustify the open loop plant G_s in the face of additive unstructured uncertainties acting on its left NCF's as presented in Section 3.3.1 (see Fig. 3.9, with K_∞ here being the robust controller K and $G_\Delta = \mathcal{F}_U(G_\mathrm{s}, \Delta)$ the perturbed plant).

As a final remark before actually giving the solution to Eq. 3.78, the maximum robustness margin $\epsilon_{\max}$ (or equivalently $\gamma_{\min}$) can be computed beforehand and before actually K_∞ and in an one step procedure for the *normalized* coprime factorization of G_s. In addition it depends *only* on the coprime factorization $[\tilde{M}, \tilde{N}]$ of G_s as[22]:

$$\epsilon_{\max} = \sqrt{1 - \left\| [\tilde{M}, \tilde{N}] \right\|_H^2}. \tag{3.79}$$

[20] For additional details see [97], Section IV or [96], Sections 6.5, 6.6.

[21] Note that now the *final* open loop plant of Theorem 3.3 is the one obtained by augmenting the *initial* open loop plant with the pre/post compensators of the LSDP of Section 3.3.2.

[22] The subscript 'H' denotes the Hankel norm of a system associated to its Hankel singular values.

3.3.3.1 Standard Solution

Consider the strictly proper[23] state space representation of the open loop shaped plant G_s (see Fig. 3.10a) satisfying the classic $\mathscr{H}_\infty$ assumptions needed (see [155], Ch. 16): Shaped system

$$G_\mathrm{s}: \quad \begin{aligned} \dot{x} &= \mathbf{A}_\mathrm{s} x + \mathbf{B}_\mathrm{s} u \\ y &= \mathbf{C}_\mathrm{s} x \end{aligned} \tag{3.80}$$

Then out of all stabilizing controllers achieving also the tolerance level γ, the so-called central or maximum entropy one K_∞ with: Feedback controller

$$K_\infty: \quad \begin{aligned} \dot{x}_k &= \mathbf{A}_k x_k + \mathbf{B}_k y \\ u &= \mathbf{C}_k x_k + \mathbf{D}_k y \end{aligned} \tag{3.81}$$

is given by:

$$\begin{aligned} K_\infty &\overset{\mathrm{ss}}{=} \begin{bmatrix} \mathbf{A}_k & \mathbf{B}_k \\ \mathbf{C}_k & \mathbf{D}_k \end{bmatrix} \\ &= \begin{bmatrix} \mathbf{A}_\mathrm{s} - \mathbf{B}_\mathrm{s}\mathbf{B}_\mathrm{s}^T\mathbf{X} + \gamma^2\mathbf{W}^{-1}\mathbf{Z}\mathbf{C}_\mathrm{s}^T\mathbf{C}_\mathrm{s} & \gamma^2\mathbf{W}^{-1}\mathbf{Z}\mathbf{C}_\mathrm{s}^T \\ {\mathbf{B}_\mathrm{s}}^T\mathbf{X} & 0 \end{bmatrix}. \end{aligned} \tag{3.82}$$

The matrices $\mathbf{X}, \mathbf{Z}$ solve the *control* (respectively *filtering*) algebraic Riccati equations (CARE, FARE):

$$\text{CARE}: \quad \mathbf{A}_\mathrm{s}^T\mathbf{X} + \mathbf{X}\mathbf{A}_\mathrm{s} - \mathbf{X}\mathbf{B}_\mathrm{s}\mathbf{B}_\mathrm{s}^T\mathbf{X} + \mathbf{C}_\mathrm{s}^T\mathbf{C}_\mathrm{s} = 0 \tag{3.83}$$

$$\text{FARE}: \quad \mathbf{Z}\mathbf{A}_\mathrm{s}^T + \mathbf{A}_\mathrm{s}\mathbf{Z} - \mathbf{Z}\mathbf{C}_\mathrm{s}^T\mathbf{C}_\mathrm{s}\mathbf{Z} + \mathbf{B}_\mathrm{s}\mathbf{B}_\mathrm{s}^T = 0 \tag{3.84}$$

with the matrix $\mathbf{W}$ (entering $\mathbf{A}_k, \mathbf{B}_k$) given by:

$$\mathbf{W} = \left(\mathbb{I} + \mathbf{X}\mathbf{Z} - \gamma^2\mathbb{I}\right)^T. \tag{3.85}$$

The maximum robustness margin ϵ_max obtained can be also calculated using the solutions $\mathbf{X}, \mathbf{Z}$ of the Riccati equations as (with $\epsilon_\mathrm{max} < 1$ always): Optimal robustness margin

$$\epsilon_\mathrm{max} = \frac{1}{\sqrt{1 + \lambda_\mathrm{max}(\mathbf{X}\mathbf{Z})}}. \tag{3.86}$$

Technical Note: The problem of designing a sub-optimal robust output feedback controller following the McFarlane & Glover loop shaping design procedure (LSDP) is solved by MATLAB® with the macro '`ncfsyn`' of the Robust Control Toolbox. This macro designs a positive feedback controller K_∞ for an open loop plant G with corresponding pre/post compensators W_1, W_2. Additionally it computes the corresponding maximum stability margin ϵ_max, the stability margin ϵ achieved and the corresponding augmented open loop plant G_s and stabilized closed loop system transfer functions.

[23] The *strictly proper* case is considered here in order to simplify the formulas.

3.3.3.2 LMI Solution

In this section an alternative method for the solution of the sub-optimal robust stabilization corresponding to the LSDP of Section 3.3.2 is presented. This method is based on a LMI formulation of the problem of finding the stabilizing robust dynamic controller K_∞ that also satisfies Eq. 3.78.

The idea is simple enough: given that the problem of designing this stabilizing controller corresponds to the minimization of the $\mathscr{H}_\infty$ norm from the input disturbance w (representing the additive uncertainty over the normalized left coprime factors of the shaped open loop plant G_s) to the performance vector ζ_∞ consisting of the input u and the output y of G_s (see Fig. 3.9); then it suffices to design the controller K_∞ for the corresponding standard plant P_s of Fig. 3.11 in such a way that $\|T_{w\zeta_\infty}\|_\infty = \|\mathcal{F}_L(\mathbb{P}_\mathrm{s}, K_\infty)\|_\infty < \gamma$ with K_∞ stabilizing and γ minimized. The solution to this problem via LMI's could be done in more than one ways; here the basic approach found in [11] is presented.

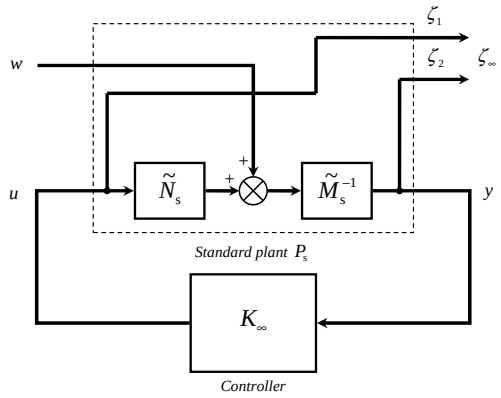

Figure 3.11: LFT of the LSDP.

To find the standard plant representation $\mathbb{P}_\mathrm{s}$ of the open loop shaped plant G_s, with a general standard plant representation defined as:

$$\begin{bmatrix} \dot{x} \\ \zeta_\infty \\ y \end{bmatrix} = \begin{bmatrix} \mathbf{A} & \mathbf{B}_w & \mathbf{B}_u \\ \mathbf{C}_\zeta & \mathbf{D}_{w\zeta} & \mathbf{D}_{u\zeta} \\ \mathbf{C}_y & \mathbf{D}_{wy} & \mathbf{D}_{uy} \end{bmatrix} \begin{bmatrix} x \\ w \\ u \end{bmatrix} \tag{3.87}$$

NCF's

it suffices to obtain a minimal normalized LCF of the shaped open loop plant $G_\mathrm{s} = \left[\begin{smallmatrix} \mathbf{A}_\mathrm{s} & \mathbf{B}_\mathrm{s} \\ \mathbf{C}_\mathrm{s} & \mathbf{D}_\mathrm{s} \end{smallmatrix}\right]$[24]. These coprime factors of are given by [155] (with $G_\mathrm{s} = \tilde{M}^{-1}\tilde{N}$):

$$\tilde{N} \overset{\text{ss}}{=} \begin{bmatrix} \mathbf{A}_\mathrm{s} + \mathbf{L}\mathbf{C}_\mathrm{s} & \mathbf{L} \\ \mathbf{R}^{-1/2}\mathbf{C}_\mathrm{s} & \mathbf{R}^{-1/2} \end{bmatrix} \tag{3.88}$$

$$\tilde{M} \overset{\text{ss}}{=} \begin{bmatrix} \mathbf{B}_\mathrm{s} + \mathbf{L}\mathbf{D}_\mathrm{s} & \mathbf{L} \\ \mathbf{R}^{-1/2}\mathbf{D}_\mathrm{s} & \mathbf{R}^{-1/2} \end{bmatrix}. \tag{3.89}$$

[24] The more general case where the plant is not necessarily strictly proper is considered here with $\mathbf{A}_\mathrm{s} \in \mathbb{R}^{n\times n}, \mathbf{B}_\mathrm{s} \in \mathbb{R}^{n\times n_u}, \mathbf{C}_\mathrm{s} \in \mathbb{R}^{n_y\times n}, \mathbf{D}_\mathrm{s} \in \mathbb{R}^{n_y\times n_u}$.

After the necessary matrix manipulations the standard plant $\mathbb{P}_\mathrm{s}$ is found to be (one-to-one connection using Eq. 3.87): LSDP standard plant

$$\mathbb{P}_\mathrm{s} \overset{\mathrm{ss}}{=} \begin{bmatrix} \mathbf{A}_\mathrm{s} & -\mathbf{L}\mathbf{R}^{1/2} & \mathbf{B}_\mathrm{s} \\ \begin{bmatrix} 0 \\ \mathbf{C}_\mathrm{s} \end{bmatrix} & \begin{bmatrix} 0 \\ \mathbf{R}^{1/2} \end{bmatrix} & \begin{bmatrix} \mathbb{I}_{n_u} \\ \mathbf{D}_\mathrm{s} \end{bmatrix} \\ \mathbf{C}_\mathrm{s} & \mathbf{R}^{1/2} & \mathbf{D}_\mathrm{s} \end{bmatrix}. \tag{3.90}$$

The coprime factorization matrices $\mathbf{R}, \mathbf{L}$ in Eq. 3.90 are defined as:

$$\mathbf{R} = \mathbb{I} + \mathbf{D}_\mathrm{s}\mathbf{D}_\mathrm{s}^T \tag{3.91}$$

$$\mathbf{L} = -\big(\mathbf{B}_\mathrm{s}\mathbf{D}_\mathrm{s}^T + \mathbf{Z}\mathbf{C}_\mathrm{s}^T\big)\mathbf{R}^{-1} \tag{3.92}$$

where $\mathbf{Z} = \mathbf{Z}^T, \mathbf{Z} > 0$ is the solution to the (generalized) *filtering* algebraic equation (GFARE):

$$\begin{aligned} \text{GFARE}: \quad \big(\mathbf{A}_\mathrm{s} - \mathbf{B}_\mathrm{s}\mathbf{S}^{-1}\mathbf{D}_\mathrm{s}^T\mathbf{C}_\mathrm{s}\big)\mathbf{Z} + \mathbf{Z}\big(\mathbf{A}_\mathrm{s} - \mathbf{B}_\mathrm{s}\mathbf{S}^{-1}\mathbf{D}_\mathrm{s}^T\mathbf{C}_\mathrm{s}\big)^T \\ -\mathbf{Z}\mathbf{C}_\mathrm{s}^T\mathbf{R}^{-1}\mathbf{C}_\mathrm{s}\mathbf{Z} + \mathbf{B}_\mathrm{s}\mathbf{S}^{-1}\mathbf{B}_\mathrm{s}^T = 0 \end{aligned} \tag{3.93}$$

and

$$\mathbf{S} = \mathbb{I} + \mathbf{D}_\mathrm{s}^T\mathbf{D}_\mathrm{s}. \tag{3.94}$$

Given the standard plant $\mathbb{P}_\mathrm{s}$ the solution to the problem of finding the dynamic controller K_∞ is divided into two phases: the *feasibility problem* and *controller reconstruction*. The first phase involves the solution of a number of LMI's, which is the result of the effort of rendering the corresponding Bounded Real Lemma (BRL) convex, in order to obtain the problem's Lyapunov matrices[25]. If these exist, then the *initial* BRL becomes convex, the second phase has a meaning and the controller matrices may be computed by solving the *initial* BRL either as an LMI problem or symbolically (for the latter method see [68]).

Feasibility Problem: The following theorem gives the necessary and sufficient conditions for the existence of a sub-optimal full order output feedback $\mathscr{H}_\infty$ controller K for a general standard plant $\mathbb{P}$ like the one of Eq. 3.87[26]: Feasibility problem

Theorem 3.4. Under the hypothesis that the pairs $(\mathbf{A}, \mathbf{B}_u)$ and $(\mathbf{A}, \mathbf{C}_\mathbf{y})$ are stabilizable and detectable then there exists a full order dynamic controller K (as the one in Eq. 3.43) ensuring that the transfer function $T_{w\zeta_\infty}(s) = \mathcal{F}_L(\mathbb{P}, K)$ from the vector of disturbances w to a performance vector ζ_∞ will be stable and also the $\mathscr{H}_\infty$-norm of this transfer function will be less than a performance level γ ($\|T_{w\zeta_\infty}\|_\infty < \gamma$), if and only if there exist symmetric matrices $\mathbf{X}, \mathbf{Y}$ and a performance level $\gamma > 0$ satisfying the following three LMI's:

[25] This is equivalent to the solution of the two Riccati equations when using the standard problem formulation of the previous section.

[26] In the following analysis it will be assumed without loss of generality that $D_{uy} = 0$ in order to simplify the calculations.

$$\begin{bmatrix} \mathcal{N}_{\mathbf{X}} & 0 \\ 0 & \mathbb{I} \end{bmatrix} \begin{bmatrix} \mathbf{A}\mathbf{X} + \mathbf{X}\mathbf{A}^T & \mathbf{X}\mathbf{C}_\zeta^T & \mathbf{B}_w \\ \mathbf{C}_\zeta \mathbf{X} & -\gamma\mathbb{I} & \mathbf{D}_{w\zeta} \\ \mathbf{B}_w^T & \mathbf{D}_{w\zeta}^T & -\gamma\mathbb{I} \end{bmatrix} \begin{bmatrix} \mathcal{N}_{\mathbf{X}} & 0 \\ 0 & \mathbb{I} \end{bmatrix} < 0 \tag{3.95}$$

$$\begin{bmatrix} \mathcal{N}_{\mathbf{Y}} & 0 \\ 0 & \mathbb{I} \end{bmatrix} \begin{bmatrix} \mathbf{A}^T\mathbf{Y} + \mathbf{Y}\mathbf{A} & \mathbf{Y}\mathbf{B}_w^T & \mathbf{C}_\zeta^T \\ \mathbf{B}_w^T \mathbf{Y} & -\gamma\mathbb{I} & \mathbf{D}_{w\zeta}^T \\ \mathbf{C}_\zeta & \mathbf{D}_{w\zeta} & -\gamma\mathbb{I} \end{bmatrix} \begin{bmatrix} \mathcal{N}_{\mathbf{Y}} & 0 \\ 0 & \mathbb{I} \end{bmatrix} < 0 \tag{3.96}$$

$$\begin{bmatrix} \mathbf{X} & \mathbb{I} \\ \mathbb{I} & \mathbf{Y} \end{bmatrix} \geq 0. \tag{3.97}$$

□

Proof. See [11], pp. 10-11.

■

The matrices $\mathcal{N}_{\mathbf{X}}, \mathcal{N}_{\mathbf{Y}}$ are (preferably orthonormal) bases to the null spaces of $\begin{bmatrix} \mathbf{B}_u^T & \mathbf{D}_{u\zeta}^T \end{bmatrix}$ and $\begin{bmatrix} \mathbf{C}_y & \mathbf{D}_{wy} \end{bmatrix}$ respectively. Now in practice, one tries to solve a minimization problem by trying to solve for the matrices $\mathbf{X}, \mathbf{Y}$ for the smallest γ possible; once this is done the controller matrices are obtained following the analysis below.

`Controller recon/tion`

Controller Reconstruction: The problem of obtaining the feasibility solutions involves in fact the convexifying of an initially BMI problem. This problem emerges by imposing satisfaction of the BRL for the closed loop system given by the l-LFT of the general standard plant $\mathbb{P}$ and the controller K. This problem can be translated into finding the matrix $\mathbf{\Theta} = \begin{bmatrix} \mathbf{A}_k & \mathbf{B}_k \\ \mathbf{C}_k & \mathbf{D}_k \end{bmatrix}$, regrouping the controller matrices, that satisfies the following inequality:

$$\mathbf{\Psi} + \mathbf{Q}^T \mathbf{\Theta}^T \mathbf{P} + \mathbf{P}^T \mathbf{\Theta} \mathbf{Q} < 0. \tag{3.98}$$

The aforementioned equation contains the matrices $\mathbf{\Psi}, \mathbf{P}, \mathbf{Q}$ that are generally dependent[27] on the known standard plant matrices *and* on $\mathbf{X}, \mathbf{Y}, \gamma$ obtained from the feasibility problem[28].

The initial problem of computing a robust dynamic controller K_∞ for the shaped open loop plant G_s can be in fact viewed as a standard $\mathscr{H}_\infty$ problem with a special structure on the corresponding standard plant $\mathbb{P}$. Given that the standard plant referring to this special problem $\mathbb{P}_\mathrm{s}$ may be computed using Eqs. 3.88-3.90, then the problem of designing K_∞ may be solved by directly applying the aforementioned LMI formulation of Theorem 3.4.

[27] For the exact dependence and how to solve for these matrices refer to [11].

[28] As a small technical note it may be added that the LMI of Eq. 3.98 can be readily solved using the macro '`basiclmi`' of the MATLAB® Robust Control Toolbox.

3.3.4 Static Case

In this section the problem of computing static instead of dynamic robust $\mathscr{H}_\infty$ controllers for the LSDP of Section 3.3.2 will be addressed. The problem in fact is to find a static output feedback control law $u = -K_\infty y$ for the shaped plant G_s of Fig. 3.10a that will stabilize the plant and also render it robust to left NCF perturbations; this is translated in the *two-block* $\mathscr{H}_\infty$ problem of Eq. 3.78 that is repeated here:

$$\left\| \begin{bmatrix} K_\infty \\ \mathbb{I} \end{bmatrix} (\mathbb{I} - G_\mathrm{s} K_\infty)^{-1} \tilde{M}^{-1} \right\|_\infty \leq \gamma, \quad \gamma > 0. \tag{3.99}$$

Static vs. dynamic $\mathscr{H}_\infty$ control

This approach of designing simpler controllers is very important in the context of gain scheduling, as it will be detailed in Chapter 6, since the controller updating procedure has a very reduced complexity. Indeed, from the discussion of Section 3.3.2 it has been made clear that the order of a dynamic controller K_s is equal to the sum of the orders of the plant plus the pre/post compensators'. Thus for example for a second order system G shaped by a PID post-compensator W_2 and a low pass filter W_1 as pre-compensator, the final controller would be of order five making things maybe more complicated than they should have been.

Two are the major solutions proposed for this problem of high controller order: the first is try to reduce the order of K_∞ (using for example techniques such as Hankel norm approximation or balanced truncation) whereas the second is attempting to compute reduced order controllers directly from the beginning; here this second method will be outlined.

The basic difficulty in designing reduced order controllers comes from the famous rank minimization condition for the existence of a controller of order $k < n$ (where n is the plant order):

$$\mathrm{Rank}(\mathbb{I} - \mathbf{XY}) \leq k. \tag{3.100}$$

Several heuristic methods have been proposed in order to take out this condition such as the alternative projection method, the XY-centering algorithm, the cone complementarity linearization method and others (see for example [52, 54] and references therein). However these approaches (along with the one trying to solve the initial problem, which is of course a BMI, with appropriate solvers) do not guarantee convergence even though they have been successfully applied to real world applications.

Other methods focus their effort to obtain only sufficient conditions for the existence of lower order controllers, conditions which however involve the formulation of the problem into LMI's. One of these methods has appeared in [111] and will be exploited in this work. Briefly, it involves the aforementioned *two-block* loop shaping problem itself and demands only the solution of two LMI's to guarantee the existence of a static controller K_∞. Another method that addresses the equivalent *four-block* problem (see Eq. 3.71) and claims to achieve better results than the previous one has been very recently proposed in [109].

Following the analysis in [111] and always under the LSDP context of the previous sections, consider the open shaped plant $G_s = \left[\begin{smallmatrix} \mathbf{A}_s & \mathbf{B}_s \\ \mathbf{C}_s & \mathbf{D}_s \end{smallmatrix}\right]$ of Figs. 3.10a-3.11. The problem this time is finding a *static* controller K_∞ and the following theorem gives sufficient conditions for the existence of such a controller.

LSDP: static $\mathscr{H}_\infty$ control feasibility

Theorem 3.5. There exist a static stabilizing controller K_∞ that also satisfies the *two-block* LSDP $\mathscr{H}_\infty$ robustness problem:

$$\left\| \begin{bmatrix} K_\infty \\ \mathbb{I} \end{bmatrix} (\mathbb{I} - G_s K_\infty)^{-1} \tilde{M}^{-1} \right\|_\infty \leq \gamma, \quad \gamma > 0.$$

if there exist $\gamma < 1$ and a matrix $\mathbf{X} = \mathbf{X}^T > 0$ that satisfies the LMI's:

$$(\mathbf{A}_s + \mathbf{L}\mathbf{C}_s)\mathbf{X} + \mathbf{X}(\mathbf{A}_s + \mathbf{L}\mathbf{C}_s)^T < 0 \tag{3.101}$$

$$\begin{bmatrix} \mathbf{A}_s\mathbf{X} + \mathbf{X}\mathbf{A}_s^T - \gamma\mathbf{B}_s\mathbf{B}_s^T & \mathbf{X}\mathbf{C}_s^T - \gamma\mathbf{B}_s\mathbf{D}_s^T & -\mathbf{L}\mathbf{E}^{1/2} \\ \mathbf{C}\mathbf{X} - \gamma\mathbf{D}_s\mathbf{B}_s^T & -\gamma\mathbf{E} & \mathbf{E}^{1/2} \\ -\mathbf{E}^{1/2}\mathbf{L}^T & \mathbf{E}^{1/2} & -\gamma\mathbb{I}_{n_y} \end{bmatrix} < 0 \tag{3.102}$$

with $\mathbf{L} = -\big(\mathbf{B}_s\mathbf{D}_s^T + \mathbf{Z}\mathbf{C}_s^T\big)\mathbf{R}^{-1}$, $\mathbf{Z} = \mathbf{Z}^T \geq 0$ being the solution to the GFARE of Eq. 3.93 and $\mathbf{R} = \mathbb{I} + \mathbf{D}_s\mathbf{D}_s^T, \mathbf{S} = \mathbb{I} + \mathbf{D}_s^T\mathbf{D}_s$.

□

Proof. See [111], pp. 1519.

■

Comments

As a first comment it should be stressed that the difficulty in computing a static controller comes from the fact that Eq. 3.101 is a BMI transformed to an LMI by neglecting an additive factor $\mathfrak{F}$ which is quadratic on $\mathbf{R}$, with $\mathfrak{F}$ being equal to[29]:

$$\mathfrak{F} = -\gamma\mathbf{R}\mathbf{C}_s^T\mathbf{E}^{-1}\mathbf{C}_s\mathbf{R}. \tag{3.103}$$

As a second comment it may be added that the procedure of arriving to the conditions of Eqs. 3.101-3.102 is nothing more than applying the standard LMI conditions of Theorem 3.4 to this particular static output feedback problem. As a result, the analysis of this section may be considered as an extension to the discussion of Section 3.3.3.2.

As a third comment it should be made clear that because of the fact that a much simpler structure controller has been designed in contrast with the full order case of the previous section, the performance level γ (respectively robustness margin ϵ) will be bigger (respectively smaller). In practice, and as it will be observed in Chapter 6, this trade-off between controller complexity and robust stability leans heavily towards the first; this meaning that the robustness margin deterioration in the static case is only about 30% for a seventh order open loop plant G_s, thus justifying the static approach.

[29] The simplification of this quadratic factor $\mathfrak{F}$ renders the conditions sufficient instead of necessary and sufficient in the beginning.

Static controller recon/tion

Now once the performance level γ and the Lyapunov matrix $\mathbf{X}$ have been found, the static output feedback gain can be computed following the *Controller Reconstruction* phase of Theorem 3.4 that involves the solution of the initial Bounded Real Lemma relevant to the problem. If $K_\infty = \tilde{K}_\infty(\mathbb{I} - \mathbf{D}_\mathrm{s}\tilde{K}_\infty)^{-1}$ then K_∞ may be computed by solving the LMI of Eq. 3.98 for $\tilde{K}_\infty$ with:

$$\mathbf{\Psi} = \begin{bmatrix} \mathbf{A}_\mathrm{s}\mathbf{X} + \mathbf{X}\mathbf{A}_\mathrm{s}^T & 0 & \mathbf{X}\mathbf{C}_\mathrm{s}^T & -\mathbf{L}\mathbf{E}^{1/2} \\ 0 & -\gamma\mathbb{I}_{n_u} & 0 & 0 \\ \mathbf{C}_\mathrm{s}\mathbf{X} & 0 & -\gamma\mathbb{I}_{n_y} & \mathbf{E}^{1/2} \\ -\mathbf{E}^{1/2}\mathbf{L}^T & 0 & \mathbf{E}^{1/2} & -\gamma\mathbb{I}_{n_y} \end{bmatrix} \tag{3.104}$$

$$\mathbf{P} = \begin{bmatrix} \mathbf{B}_\mathrm{s} \\ \mathbb{I}_{n_u} \\ \mathbf{D}_\mathrm{s} \\ 0 \end{bmatrix}^T \tag{3.105}$$

$$\mathbf{Q} = \begin{bmatrix} \mathbf{C}_\mathrm{s}\mathbf{X} & 0 & 0 & \mathbf{E}^{1/2} \end{bmatrix}. \tag{3.106}$$

This concludes the discussion on the classic LSDP of McFarlane&Glover and on how to obtain full order or static controllers using the standard Glover&Doyle formulation or an alternative LMI approach. As a last comment it may be added that this LSDP analyzed in the last sections offers indeed a sound and theoretically justified approach but which on the same time preserves its intuitive nature concerning the synthesis of MIMO controllers for LTI plants. From the one side it can encompass many interesting features that could be useful for a control system (low/high open loop gains at high/low frequencies, treatment for the general I/O disturbance rejection problem, stabilization over unstructured uncertainties etc.) but on the other hand it can be seen, in the context of singular value shaping, as a generalization to well known loop shaping practices. In addition this synthesis procedure can be further simplified by considering *simpler* control structures for the robust closed loop controller; this fact is easily done due to the fact that the LSDP can be recast as a standard $\mathscr{H}_\infty$ synthesis problem.

3.4 The Gap Metric

In this section a powerful system analysis tool will be presented that will permit the development of advanced gain scheduling controllers in Chapter 6. This tool is called *the gap metric* and it has been primarily introduced in the control community with the work of El-Sakkary in the 80's [38, 39]. It has been mostly exploited by Georgiou&Smith both concerning computational aspects and its connection with $\mathscr{H}_\infty$ control [49, 50]. Other interesting metrics were conceived by Vidyasagar [143] and more recently by Vinnicombe [146]. Additional work in a nonlinear context has been done for example in [51] and in [34] for the LTV case.

3.4.1 Motivation & Definitions

Distance between systems

A major motivation for the development of the gap metric and other metrics was the desire to obtain a measure of the distance between two systems in a *closed loop* setting and the possible extension of this idea to study the stability of a perturbed system $G_\Delta(s)$ given that it is controlled by the same compensator $K(s)$ computed for a nominal system $G(s)$. Moreover this metric should be able to compare different types of systems: stable or unstable, of the same or different orders etc.; the only restriction is that they should have the same number of inputs or outputs since they are compared in the same closed loop setting (i.e. using the same compensator).

The gap metric captures differences between the closed loop behaviors of two plants $G(s), G_\Delta(s)$ when the same compensator $K(s)$ is applied. If another system $G^*(s)$ is considered, that may have similar *open loop* but very different *closed loop* when compared to G (always with the same compensator K), then this metric should be able to distinguish G^* from G_Δ which behaves well/similarly as G in *closed loop*, though it may be totally different in *open loop*[30]. As an illustrative example suppose that G is a stable first-order system, G_Δ an unstable one, whereas G^* is similar to G in terms of open loop step response:

$$G(s) = \frac{100}{2s+1},\ G_\Delta(s) = \frac{100}{2s-1},\ G^*(s) = \frac{100}{(s+1)^2}. \tag{3.107}$$

Suppose also that all plants are given a unity negative feedback ($K(s) = -1$); then their closed loop transfer functions $H(s), H_\Delta(s), H^*(s)$ are:

$$H(s) = \frac{100}{2s+101},\ H_\Delta(s) = \frac{100}{2s+99},\ H^*(s) = \frac{100}{s^2+2s+101} \tag{3.108}$$

and all open and closed loop step responses are shown in Figs. 3.12a, 3.12b.

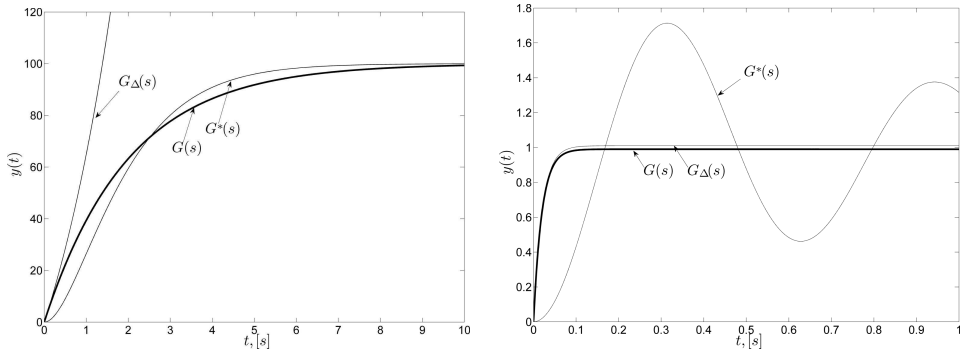

(a) *Open loop step responses* **(b)** *Closed loop step responses*

Figure 3.12: System responses comparison.

[30]For example G may be stable and G_Δ unstable in open loop as it is the case in real life situations when a nominal but uncertain plant may become unstable under heavy perturbations.

The graph topology

The topology inducing the gap metric is depicted in Fig. 3.13; this topology takes into account the special structure of the feedback problem seen in Section 3.3. In this structure, a nominal plant G that is stabilized by a compensator K, receives input/output perturbations d, n whereas another plant G_Δ, receives the same perturbations while being in feedback interconnection with the same compensator K. The goal then is to find a distance measure for the inputs/output behaviors of each system G, G_Δ under this specific feedback form. This distance measure, that is defined for these two systems G, G_Δ, is called *the gap metric* $\delta_{\mathrm{g}}(G, G_\Delta)$ and it is the maximum of the two *directed gaps* $\vec{\delta}_{\mathrm{g}}(G, G_\delta), \vec{\delta}_{\mathrm{g}}(G_\Delta, G)$:

$$\delta_{\mathrm{g}}(G, G_\Delta) \triangleq \max\left\{\vec{\delta}_g(G, G_\Delta), \vec{\delta}_g(G_\Delta, G)\right\}. \tag{3.109}$$

In this closed loop structure of Fig. 3.13, the two systems G, G_Δ may be considered close if for all *appropriate* inputs u to the plant G there exists an *appropriate* input u_Δ that makes a certain norm small. This norm, being of key importance, can be found in the actual definition of the *directed gap* between two systems which is the following:

$$\vec{\delta}_{\mathrm{g}}(G, G_\Delta) \triangleq \sup_{\begin{bmatrix} u \\ y \end{bmatrix} \in \mathcal{G}_G} \inf_{\begin{bmatrix} u_\Delta \\ y_\Delta \end{bmatrix} \in \mathcal{G}_{G_\Delta}} \frac{\left\| \begin{bmatrix} y \\ u \end{bmatrix} - \begin{bmatrix} y_\Delta \\ u_\Delta \end{bmatrix} \right\|_2}{\left\| \begin{bmatrix} y \\ u \end{bmatrix} \right\|_2}. \tag{3.110}$$

These *appropriate* inputs u, u_Δ mentioned before, along with the corresponding outputs $y = Gu, y_\Delta = G_\Delta u_\Delta$ are said to belong to the *domain* $\mathcal{D}(\mathbf{M}_G)$ of a *multiplication operator* $\mathbf{M}_G$. This *domain* is defined as:

$$\mathcal{D}(\mathbf{M}_G) \triangleq \{u \in \mathscr{H}_2 : Gu \in \mathscr{H}_2\}. \tag{3.111}$$

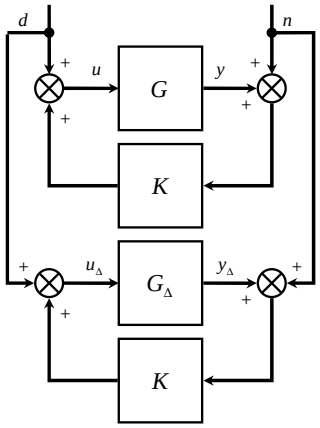

Figure 3.13: Gap metric related topology

The multiplication operator $\mathbf{M}_G$ is an operator on the input signal space $\mathcal{H}_2$, defining the signals being zero for $t < 0$ and with bounded energy for $t > 0$, and is described as:

$$\mathbf{M}_G : \mathscr{H}_2 \to \mathscr{H}_2,\ u \mapsto Gy. \tag{3.112}$$

where the system G belongs to the class of rational transfer functions with n_u inputs and n_y outputs respectively.

Returning to the definition of the directed gap of Eq. 3.110, it may be added that the gap metric can be also viewed as the distance between the so-called *graphs* of the two systems $\mathcal{G}_G, \mathcal{G}_{G_\Delta}$; this is the reason because it is a metric induced by the *graph topology*. Given that a system G may be seen as a multiplication operator $\mathbf{M}_G$, the graph of a system is defined as all the possible $\mathscr{H}_2$-bounded input/output pairs of the corresponding to G multiplication operator $\mathbf{M}_G$:

$$\mathcal{G}_G \equiv \mathcal{G}(\mathbf{M}_G) \triangleq \left\{ \begin{bmatrix} y \\ u \end{bmatrix} : u \in \mathcal{D}(\mathbf{M}_G) \right\}. \tag{3.113}$$

Gap metric properties

A very useful property of the gap metric δ_g, defined in Eq. 3.109 by means of the directed gap, is that given it is a metric the following hold[31]:

$$0 \leq \delta_g(G, G_\Delta) \leq 1 \tag{3.114}$$

and also:

$$\delta_g(G, G_\Delta) \equiv \delta_g(G_\Delta, G). \tag{3.115}$$

Returning to the initial motivation example, given that the gap metric shows the *closed loop closeness* between two systems under the same feedback structure, the gaps between all the systems are seen in Table 4.1. On the one hand it is verified that even though the systems G, G^* have similar open loop step responses (see Fig. 3.12a) their gap is large, showing exactly the incompatibility of the controller K for G^* in closed loop (see Fig. 3.12b). On the other hand, even though the open loop step response of G_Δ is unstable, therefore very different to the one corresponding to G, their gap is small since the compensator K is very good for both systems under the graph topology. In addition, because of the fact that G, G_Δ are very close by means of the gap whereas G, G^* are not, it is expected that the gap between G_Δ, G^* will be also large.

Table 3.1: Gaps concerning the motivation example.

System	$G(s)$	$G_\Delta(s)$	$G^*(s)$
$G(s)$	0	0.0205	0.8995
$G_\Delta(s)$	0.0205	0	0.8946
$G^*(s)$	0.8995	0.8946	0

[31] A large gap between two systems means that they are not close in the graph topology whereas a gap close to zero shows closed loop compatibility for an appropriate compensator K.

3.4.2 Connection to the $\mathscr{H}_\infty$ Theory

In this section the connection of the gap metric and the $\mathscr{H}_\infty$ loop shaping theory of Section 3.3 will be outlined. This important result obtained by Georgiou&Smith in [50] is of key interest since two systems G, G_Δ may be compared in a closed loop setting as in Fig. 3.13, with the second system G_Δ considered as a coprime factor perturbed of the initial one G. Quantitative results are then obtained on the maximum amount of uncertainty Δ that can be tolerated over G until the behavior of its closed loop starts to deteriorate rapidly.

The theory presented assumes *normalized* coprime factorizations of an open loop plant G and a stabilizing controller K which stabilizes and renders G robust over unstructured additive uncertainties Δ on its normalized coprime factors, exactly as in the setting of Fig. 3.9. It is argued by Georgiou&Smith that iff the $\mathscr{H}_\infty$-norm of the uncertainty introduced is less than the gap between the systems G, G_Δ then K stabilizes the perturbed system G_Δ. This result is formally given by the following theorem:

Gap metric & robust stab/tion

Theorem 3.6. Consider a system G with a *right* normalized coprime factorization $G = NM^{-1}$ and a controller K that stabilizes it. Take a real number ϵ so that $0 \leq \epsilon \leq 1$. Then these two statements are equivalent:

a. The closed loop pair $[G_\Delta, K]$ is stable for every plant G_Δ with $G_\Delta \triangleq (N + \Delta_N)(M + \Delta_M)^{-1}$ being a *right* NCF perturbed plant G, where $\Delta_N, \Delta_N \in \mathbb{R}\mathcal{H}_\infty$ and $\left\| \left[\begin{smallmatrix} \Delta_M \\ \Delta_N \end{smallmatrix} \right] \right\|_\infty < \epsilon$.

b. The closed loop pair $[G_\Delta, K]$ is stable for every plant G_Δ for which $\delta_{\mathrm{g}}(G, G_\Delta) < \epsilon$.

□

Proof. See [50], pp. 679.

■

Right vs. *left* NCF's

Now it is interesting to note that the theorem above is given in terms of *right* NCF's whereas the formulation of the robust stabilization problem stated in Theorem 3.3 is done in terms of *left* NCF's. It follows from the analysis in [50] that a controller K, being optimal for coprime factor perturbations, is optimal for both left *and* right factorizations of the plant G, even though these two types of uncertainty generate in general different classes of perturbed plants.

Given now that this controller K is optimal for both types of uncertainties, the connection with the $\mathscr{H}_\infty$ loop shaping theory is clear: a (sub)optimal controller K robustly stabilizes a plant G if the conditions of Theorem 3.3 hold, roughly if it satisfies (recall that $\mathbb{P}$ is the corresponding to G standard plant):

$$\|\mathcal{F}_L(\mathbb{P}, K)\|_\infty = \left\| \begin{bmatrix} K(\mathbb{I} - GK)^{-1}\tilde{M}^{-1} \\ (\mathbb{I} - GK)^{-1}\tilde{M}^{-1} \end{bmatrix} \right\|_\infty \leq \epsilon^{-1}. \tag{3.116}$$

Discussion on the gap

Then a simple and qualitative condition to verify if this controller K stabilizes a NCF perturbed plant G_Δ is to check whether the gap between G, G_Δ is less than the stability margin ϵ. Thus a compensator stabilizes a ball of uncertainty in the gap metric of given radius iff it stabilizes a ball of uncertainty of the same radius defined by perturbations on a normalized left coprime fraction.

It should be made clear that a perturbed plant at a distance *greater* than the stability margin will not necessarily be *destabilized* by some compensator that stabilizes the nominal plant with a stability margin equal to the gap between the two systems. This latter feature is the property of another metric: the ν-gap metric proposed by Vinnicombe in [145, 146].

As a last comment it should be added that this analysis can be extended in the context of the LSDP of Section 3.3.2. This means that the plants considered for the gap metric calculation are G_s (initial open loop plant) and $G_{\mathrm{s},\Delta}$ (the left NCF perturbed plant) with the robust controller K_∞ calculated for G_s.

3.4.3 Computation of the Gap Metric

In this final section the problem of actually computing the gap metric between two systems will be briefly addressed. For more details on the mathematics and on the method used to actually calculate the gap, the reader is encouraged to refer to [49, 50].

Computation of the gap

Even though the gap metric was introduced in [39], its actual computation for any given plants G, G_Δ was obtained by Georgiou&Smith in [49]. This is done first by noting that the gap metric $\delta_\mathrm{g}(G, G_\Delta)$ is computed as the maximum of the two directed gaps as in Eq. 3.109. Then, a quantitative expression for computing the directed gap stems from Eq. 3.110 by using the Commutant Lifting Theorem (see [50], pp. 674 and references therein):

$$\vec{\delta}_\mathrm{g}(G, G_\Delta) = \inf_{Q \in \mathscr{H}_\infty} \left\| \begin{bmatrix} M_G \\ N_G \end{bmatrix} - \begin{bmatrix} M_{G_\Delta} \\ N_{G_\Delta} \end{bmatrix} Q \right\|_\infty . \tag{3.117}$$

In the above equation M_i, N_i are right NCF of any plant G_i[32] and Q is related to the Youla parametrization procedure of any stabilizing controller K acting on G. Even though this equation does not give on its own any clear way on how to compute the gap, it may be further manipulated in order to conceive a traceable algorithm for this computation and it was a milestone getting a quantitative method to transform the graph topology-induced metric (see Eq. 3.110) into the exploitable expression in Eq. 3.117.

Technical Note: The gap metric and the ν-gap metric can be calculated to any desired accuracy by using MATLAB® Robust Control Toolbox and the command '`gapmetric`'. The calculation time needed is small enough (typically less than 500ms) to permit its use inside a robustness verification algorithm as it will be seen in Chapter 6.

[32] Recall that $G_i(s) \triangleq N_i(s) M_i^{-1}(s)$ and $M_i^* M_i + N_i^* N_i = \mathbb{I}$, with $M_i, N_i \in \mathbb{R}\mathcal{H}_\infty$.

3.5 Conclusions

In this chapter some topics of modern $\mathscr{H}_\infty$ theory were presented in order to give insights and to provide completeness in the technical part of this work.

In Section 3.1 the general framework of output feedback $\mathscr{H}_\infty$ control with pole placement in LMI regions was presented. It has been argued that this control synthesis approach is attractive since it permits the tailoring of the plant's closed loop dynamics in terms of eigenvalue placement, along with $\mathscr{H}_\infty$-based optimization on several closed loop objectives. The disadvantage of this method is the complexity of the controller obtained when full order convex synthesis is assumed.

In Section 3.2 some standard results on how to transform an arbitrary compensator into an equivalent observer-based state feedback controller were reviewed. It has been argued that in order to simplify the control structure in the context of linearization-based gain-scheduled control, it is preferable to consider strictly proper compensators with order equal to that of the plant in order to obtain a null Youla parameter Q. A drawback of this method is that the partition of the closed loop eigenvalues to the state feedback or the observer part of the controller is sometimes not so trivial.

In Section 3.3 some material on the classic McFarlane&Glover loop shaping design procedure (LSDP) was detailed. The problem of coprime factor robustness stabilization was also linked to the LSDP and the solution with a robust, either full order or static, controller was presented. The discussion involved the result that this procedure is particularly attractive in the context of gain scheduling control for two reasons: first it offers an intuitive but theoretically justified procedure of computing high performance controllers based on frequency domain analysis and second because it gives the means to link stability of a plant as a function of the uncertainty introduced on its coprime factors.

In Section 3.4 finally, a tool (the gap metric) linking stability and uncertainty was presented. The gap metric is in fact a norm under a closed loop feedback setting and it can give information on the stabilizability of a NCF perturbed plant by a controller computed for a nominal plant. With this tool the classic LSDP can be linked with gain scheduling as it will be seen in Chapter 6: a LTI plant calculated around an equilibrium point near (or not too near) another 'nominal' one may be seen as a 'perturbed' plant. Thus the gap between these two plants could give valuable information on the stabilizability of the second plant using a controller calculated for the nominal one.